AD 292 016

TECHNICAL INFORMATION SERIES

(1)

R62SD56

SHOCK TUNNEL STUDIES OF THE AERODYNAMICS OF ATMOSPHERIC ENTRY

W.R.WARREN
E.M.KAEGI
C.J.HARRIS
R.E.GEIGER

SPACE SCIENCES LABORATORY

GENERAL ELECTRIC

MISSILE AND SPACE DIVISION

SPACE SCIENCES LABORATORY

ADVANCED AERODYNAMICS OPERATION

SHOCK TUNNEL STUDIES OF THE AERODYNAMICS OF ATMOSPHERIC ENTRY

by

W. R. Warren
E. M. Kaegi
C. J. Harris
R. E. Geiger

Originally presented at the ARS 15th Annual Meeting, Washington, D. C., December 5-8, 1960

R62SD56 - Class I
May, 1962

MISSILE AND SPACE VEHICLE DEPARTMENT

GENERAL ELECTRIC

SUMMARY

The shock tunnel is an aerodynamic test facility that is capable of producing gas flows at temperature, Mach number and pressure level combinations beyond the reach of more standard laboratory tools. Therefore, it is attractive as a test device for the study of the aerodynamic problems of current and future atmospheric entry vehicles. To illustrate this, the nature of several of these problems and the performance characteristics of the shock tunnel are discussed.

The conduction of meaningful aerodynamic experiments in shock tunnel test flows depends largely upon, first, the availability of satisfactory instrumentation techniques, and second, a knowledge of the properties of the test section flows. The main objective of this paper is to present the results of recent work in these areas obtained in the General Electric shock tunnel.

The MSVD shock tunnel has a six inch diameter driven tube and a 30 inch diameter test section. To date, experiments have been conducted exclusively in air over a Mach number range of 5 to 24, a free stream Reynolds number range of 10^2 to 10^6 per inch, and a stagnation temperature range of 1200° to 6300°K. The design and operating characteristics of the facility are described briefly.

The five major test instrumentation techniques used in the tunnel are described. These allow the measurement of the following types of model data: (1) surface pressure distributions, through the use of small piezoelectric crystal gages and special mounting and calibration techniques, (2) surface heat transfer distributions, through the use of thin film resistance thermometers (quantitative) and scorch models (qualitative), (3) aerodynamic forces and moments, through the use of the optical tracking of light models that are allowed to fly freely in the test flow, (4) flow field geometries through the use of high speed schlieren and shadowgraph techniques, and (5) boundary layer flow directions, inferred from surface oil streak studies. Typical experimental results are presented and discussed.

Results from studies designed to study the quality of the test section flow are described. Considered are the departures from equilibrium in expanding high temperature nozzle flows, the thickness, predictability, and establishment of the nozzle boundary layer, the rapidity of test flow establishment, the effects of quasi-steady flows, the uniformity of test section flow properties and their agreement with theoretical predictions, and the effects of flow divergence in the conical nozzle.

The need for improvements in shock tunnel capabilities, based upon the current performance limits and future study requirements, and possible methods for implementing these improvements are discussed briefly.

CONTENTS

I. INTRODUCTION

Interest in the field of high speed aerodynamics has continued to increase in recent years largely because of our expanding concern with high performance atmospheric entry vehicles. The general success in the ICBM and satellite re-entry fields has shown that there are no insurmountable problems associated with atmospheric entry. However, as we progress to more advanced mission objectives we can see that there is still much to learn in the high speed aerodynamics field if we are ever to achieve the sophistication and reliability of design that we now enjoy in the subsonic and supersonic flight regimes.

Not only are the problems of advanced vehicles significantly more complicated than those of the earlier re-entry vehicles, but by their nature (e.g., three dimensional mixed viscous and invicid flows) they are less amenable to analytical attack. It is clearly indicated, therefore, that emphasis must be placed on the experimental approach. The spectrum of experimental studies can vary from relatively small scale laboratory investigations to large and full scale tests in large facilities and free flight programs. The former are primarily for the investigation, over wide ranges of variables, of new problems and for the verification of analytical approaches, while the latter are for the verification of design techniques and reliability as well as for the investigation of certain problems that cannot be well studied in a ground facility.

The recognition of the importance of laboratory studies in the hypersonic flow regime has led to the accelerated development of several advanced laboratory facilities. These include shock tunnels, hot shot tunnels, electric arc heated facilities, high Mach number helium tunnels, hypervelocity aerodynamic ranges, and continuous flow hypersonic tunnels at Mach numbers well above 10. The purpose of this paper is not to discuss the advantages and disadvantages of the different facilities, but to present the performance capabilities of the shock tunnel in relation to the requirements of atmospheric entry flight aerodynamic problems.

References 1 through 6 present a cross section of the work that has been done on the development of shock tunnel facilities in this country. Briefly, the shock tunnel can be described as a blow-down wind tunnel in which the working gas is heated and compressed by a shock tube flow. The conceptual simplicity and flexibility of the shock tube make available broad ranges of aerodynamic flow properties in the tunnel's test section. This has been one of its major advantages. Of course, the shock tunnel is limited to short testing times - the order of a millisecond - and this prevents its application to the study of certain problems of atmospheric entry. For example, the properties of heat protection systems cannot be studied except on a very limited basis.

II. OPERATION AND PERFORMANCE

The shock tunnel shown in Figures 1 and 2 (refs. 5, 6, 7) has a 30" diameter test section, a 6" i.d., 112' long driven tube, and an 8" i.d. combustion driver, 22' long. The test flow nozzle shown in Figure 1 is conical in shape with a 15^{o} half angle and, although this has disadvantages in certain types of testing, it affords the practical advantage of wide test condition flexibility; that is, simply by changing nozzle throats and operating at different pressure levels, the test conditions can be varied over wide ranges of variables.

The combustion driving technique employed in this facility uses an initial 70% helium-30% stoichiometric hydrogen and oxygen mixture. This driver has been found to be highly satisfactory on the basis of performance, repeatability, and reliability. Good combustion performance has been obtained to pressures of approximately 11,000 psi (ref. 5), although the tunnel is seldom operated at levels above half that value.

Experiments may be conducted in three regions of flow. These are shown in Figure 1. In the non-reflected and straight tube test regions, the test (driven) gas flows downstream behind the incident shock wave and over the models (expanding to a moderate flow Mach number in the nozzle case). A steady or quasi-steady test flow is established quickly and exists for a millisecond or less. The test flow is terminated generally in these types of tests when the diffuse boundary between the driven gas and the driver gas reaches the model. For the reflected nozzle case, a shock wave moves upstream after the incident wave reaches the end of the driven tube and essentially stagnates the test gas. The doubly shocked air then expands through the throat, nozzle, and test section and into the dump tank, which is of a sufficiently large volume and at low enough initial pressures to preclude the necessity of a pressure recovery design. The test time in this case is longer (approximately 1 - 5 milliseconds) than in the other test regions, and it is generally terminated by the arrival of waves in the nozzle that appreciably change the flow conditions. The tailored interface method of operation (ref. 8), which eliminates the first test time restricting wave in the usual shock tunnel process, allows the use of a shorter tube and provides somewhat longer test times than does standard reflected nozzle operation; however, it is not used standardly in the MSVD shock tunnel, since appreciable test times are desired in the non-reflected nozzle operation (requiring a long driven tube) and since only a small range of operating incident shock Mach numbers are available with effective tailoring with a combustion driver of the type used.

In the two nozzle flows, some means must be used to accelerate the starting waves, generated by the intersection of the incident shock wave and the nozzle, through the nozzle so that a large percentage of the test

time is not lost. This can be done through the use of a second diaphragm at the nozzle entrance which separates the initial driven tube pressure level from a much lower level in the nozzle and dump tank (ref. 9). In practice, however, the use of any simple diaphragms (e. g. mylar) have been unsatisfactory because of the damage done to models and instrumentation during the test time. A satisfactory solution to this problem has been developed in the non-reflected nozzle, through the use both of helium in the nozzle and dump tank at a pressure level equal to the initial value in the driven tube (p_1) and of a quick opening gate valve that is actuated just before a test. In the reflected nozzle, flow is started through the use of either a mechanically removed nozzle stopper (again actuated just before a run) or of an "unbalanced" mylar diaphragm located just downstream of the throat (Fig. 1). Most tests to date have been in the two tunnel configurations, i. e., the reflected and the non-reflected nozzles. Each test condition has specific advantages as discussed below.

In Fig. 3a is shown a performance map of the shock tunnel. Here we have considered only the reflected and non-reflected nozzles. The wide range of flow Mach numbers are obtained in the reflected nozzle. The line of operation to the left is for the non-reflected nozzle in the MSVD shock tunnel facility. As shown in Fig. 1 this nozzle is restricted to one geometric area ratio ($A_1/A_2=25$) and serves the purpose of providing certain specialized test conditions. The detailed operation map in Fig. 3a is for a driver pressure level, after combustion, of approximately 3,000 psi, a standard operating condition for the facility. The various Mach and Reynolds number combinations in the test sections are obtained with this driver by varying the nozzle area ratio (the throat diameter) and the initial pressure in the driven tube (p_1). The map was obtained by combining theoretically and experimentally determined information; that is, the flow properties of the test section are calculated results, based upon measured effective nozzle area ratios, incident Mach numbers, and driven tube initial pressure levels. The theoretical results are based on an extensive series of calculations performed over a wide range of flow conditions and for air in thermodynamic and chemical equilibrium (ref. 10).

The boundaries of the performance map will vary roughly in proportion to the final driven tube pressure. To illustrate this point, boundaries for higher and lower driver pressures are sketched in Figs. 3a and 3b. At the higher driver pressure, the upper Reynolds number boundary is determined by a stress limitation in the reflected region of the shock tube. Another limit on the extension of operation to the low-temperature, high Mach number regions is the condensation temperature limit of the expanding gas(ref. 12). It is difficult to specify this limit accurately. From pitot pressure surveys, Thomas and Lee (ref. 13) have shown satisfactory operation to static temperatures of 31°K at a Mach number of 11. 4. In the shock tunnel,

comparisons of model surface pressure data at Mach number of 17.5 (ref. 14) have failed to show any significant differences for free stream static temperatures of 38°K and 60°K. For higher Mach number operation it may be possible to expand to significantly lower temperatures; it appears that considerably more work is required to define the limits for condensation in hypersonic nozzles and to determine what effects condensation has on experimental results.

Flow properties for constant area ratio nozzles are shown in Fig. 3a. It is seen that as the total temperature of a flow in a given nozzle is increased, the Mach number drops rapidly. This is a result of the increase of the number of degrees of freedom in the gas which reduces the effective γ of the expanding gas.

Some other important properties for the specification of test conditions in relation to the environment requirements of a problem under consideration are given in Figs. 3a and 3b. These are the electron concentration in the stagnation region of a blunt body at the test section, the free stream mean free path of the test section flow (ref. 11), and a modified $\overline{x}$ factor.

III. PROBLEM CLASSIFICATION AND SIMULATION

Figure 4 presents an operating range map outline on which are superimposed several typical atmospheric entry vehicle trajectories (ref. 15). It is included to show that not only are the properties available in the shock tunnel test section in the regions of interest of the intended application - the study of atmosphereic entry problems - but also that they do not provide complete simulation of important flow parameters over certain vehicle operation ranges. This simple comparison is not sufficient, however, to justify or preclude the use of the shock tunnel; one must look more deeply, first, into the nature of the problems encountered and, second, into the ability of the shock tunnel to provide satisfactory flows at conditions within the sensitivity limits of its instrumentation. In other words, the ability to study each specific problem in the shock tunnel must be judged according to its own simulation requirements; it is often found that the simulation requirements on several parameters can be relaxed without reducing the value of the experiment or preventing the application of its results to design studies. Analytical and previous experimental results are important in establishing the requirements of each study. In being able to divide the general problem area into several different problem areas, we are indicating that this approach has been successful.

An attempt has been made to classify the aerodynamic problems in which we are interested. This listing is given in Table 1. Of course, any classification of such a broad problem area must be somewhat arbitrary, since different sub-problems can be grouped in several ways. Six problem areas have been called out, each of which can be studied to a greater or lesser degree in the shock tunnel. In the first, lifting vehicle aerodynamic characteristics, we are interested in determining the force and moment characteristics of new classes of body shapes and in developing understanding of the specific heat transfer problems associated with them. To conduct studies here we need, primarily, wide Mach and Reynolds number ranges and, therefore, a wide $\overline{\chi}$ range. A moderate stagnation temperature range is also desirable to help in determining boundary layer effects upon the characteristics investigated. Shapes in which we are interested correspond to low L/D (0 to 1.0 approximately) through high L/D (to the order of 3.0) configurations. They must be studied over wide angle of attack ranges; therefore, the flow fields are highly three dimensional. Another important consideration is that for the higher L/D and lower weight vehicles that are attractive for manned entry, viscous forces can play an important part in determining properties of the flows. In the study of the problems of ballistic vehicle aerodynamic characteristics, the second item in Table 1, the same types of simulation considerations exist. Here the flows are less determined by three-dimensional considerations so that more reliance may be placed

upon available analytical techniques. Problems that may be classed under hypersonic flow studies are by their nature quite similar to those in the first two categories. However, we have a tendency to group in this category the more basic, or at least more detailed, investigations of the phenomena that are encountered at high Mach number flight conditions. We have defined three broad sub-problem areas; inviscid flows, referring to induced effects generated by curved shock waves, interaction effects, referring to the interaction of boundary layers and shock waves in the more or less continuum flow regime, and separated flows. Here, approximately the same Mach and Reynolds number (and $\bar{x}$) variations as discussed previously, are required; however because of the interest in determining the basic nature of the flows being studied, it is believed that a wider stagnation temperature (or total enthalpy) range is required in order to study the effect of this variable. The low density aerodynamics area might well be included under hypersonic flow studies. Here we refer to flows in which strong boundary layer and shock wave interactions are obtained, that is, where we obtain complete merging of the body bow shock wave and surface boundary layer. Under this heading, we are also concerned with appreciable slip flow effects near the leading edge.

In general, the four areas just discussed require high Mach number - i.e., reflected nozzle-test conditions for their investigation. (In the study of problems in which the surface boundary layer is turbulent however, the low Mach number - high Reynolds number test condition of the non-reflected nozzle is useful. In these cases it is usually permissible to relax the free stream Mach number simulation, since the properties of flows near the surfaces of shapes of interest are often not strongly dependent on Mach number.) The next two areas in Table 1 can be investigated at relatively low Mach numbers (the order of 5). Since the study of these problems at times requires a high gas density, it is seen that the non-reflected nozzle can be used to good advantage. Here, test conditions of high temperatures, high densities, and therefore, high electron concentrations and large electron neutral collision frequencies are available. Investigations may be conducted in which relative effects of applied magnetic fields or microwave radiation may be determined with reasonable aerodynamic simulation. We also observe that the relaxation of high Mach number simulation becomes less of a disadvantage when studying local effects in these problem areas, since body shapes may be varied to increase local flow scaling towards full scale flight conditions. For example, when investigating problems of electromagnetic wave transmission and energy coupling with the slightly ionized plasmas around blunt bodies, the size and performance range of this facility would prevent full-scale simulation in some regions of interest. However, by generating a flow field which simulates the more important parameters such as collision frequencies and electron densities, with dimensional gradients comparable to the case of interest, one can relax some of the aerodynamic simulation and still perform a useful experiment. Such a technique requires a detailed knowledge of the flow field properties which may be calculated by methods discussed in reference 16. Another

advantage of the non-reflected nozzle for studies of this type is that the expansion non-equilibrium problem is reduced for some operating conditions, since the gas is not stagnated after the energy addition by the incident shock wave as it is in the reflected nozzle. Eschenroder and Daiber (ref. 17) have shown, for reflected nozzle reservoir conditions of 4000^{0}K, 100 and 1000 atmospheres, that freezing would begin close to the throat for nozzle dimensions of interest. Similar test conditions can be developed with a straight through nozzle expansion using incident shock wave strengths of approximately $M_s = 7.5$ into initial driven tube pressures (P_1) above 200 mm. At these conditions the region 2 gas would equilibriate quite rapidly. As its flow is already above Mach number 2, freezing of the electron concentrations would be expected to occur at significantly lower values than in a reflected nozzle. For generating flow conditions comparable to reflected nozzle operation with reservoir conditions of 8000^{0}K, 100 and 1000 atmospheres, reference 17 indicates no significant improvement in straight-through nozzle operation, since freezing occurs farther downstream in the reflected case. To more accurately compare the electron densities for the two nozzle configurations, it would be necessary to calculate all the flow properties using finite reaction rates (ref. 18). Of course, in cases where low density effects are important (Hall current influence on the performance of MHD systems, for example), studies can be made in the reflected nozzle with its improved Mach number simulation capabilities. However, one must be concerned with the possibility that non-equilibrium effects might distort the flow picture. Analyses such as reported in reference 19 provide some insight into these effects on the blunt body stagnation properties. Their dependancy on knowledge of reaction rates and certain simplifying assumptions still requires experimental verification. To this end, the application of diagnostic techniques such as those discussed in reference 20 will enable the measurement of several important species properties.

In Figure 5 an attempt has been made to specify the shock tunnel operational areas over which these various problems can be studied. Again, this is somewhat arbitrary as in the classification of the problem areas themselves. However, we feel that it does indicate the flexibility of the shock tunnel as a tool for the study of problems important in atmospheric entry aerodynamics.

IV. INSTRUMENTATION TECHNIQUES

A summary of model instrumentation techniques is given in Table 2. These techniques are used to obtain aerodynamic data in the test section of the shock tunnel. Several new techniques designed to measure important properties of a flowing high temperature gas are now under development and are described in reference 20. Other instrumentation methods used to monitor the flow in the shock tube portion of the facility, are discussed in reference 6.

Fig. 5 lists five principle techniques. Model surface pressure distributions are measured through the use of piezoelectric crystal gage (ref. 21); these are shock mounted to reduce vibration effects and are located in a small flow cavity to reduce initial loading rate effects. Two types of gages are currently in use (see Fig. 6). First, a commercially available quartz crystal gage is used at pressure levels of 0.1 psi and above. When equipped with a protecting adaptor section, this gage has measured pressures above 10,000 psi in the driver of the shock tube. Because of its large size, it is used only when a large number of points on a model are not required. The second gage is also available commercially; it contains a barium titanate crystal as a sensing element. This material is more sensitive than quartz (readable measurements have been obtained at the .0005 psi level); however, it must be calibrated dynamically. The quartz gages may be calibrated in a static test set-up. Dynamic calibrations for the pressure gages are conducted at low M_s values in a small instrumentation shock tube.

Surface heat transfer rates are measured through the use of two different resistance thermometer techniques. The first, more generally used method employs quartz plugs upon which are sputtered thin films of platinum approximately .15 microns thick. The film is then used as a resistance thermometer, and the surface temperature history of the quartz is measured during a shock tunnel run. This technique is used for heating rates below approximately 1,000 Btu/ft^2-sec. At higher values the thick film technique is employed. Here a strip of ferrous alloy, sufficiently thick to insure negligible heat losses at the rear surface, is employed essentially as a calorimeter gage. While the thin film gages must be replaced frequently, the thick film gages are durable and may be used repeatedly. The response time of each gage is of the order of microseconds. This is sufficiently short to assure accurate heat transfer rate measurements during the test time. Figure 7 presents a photograph of three thin film heat transfer gages next to a typical model. Inserted into Fig. 7 are an oscilloscope trace record from a run in the shock tunnel and the reduced heat transfer rate history for that record. The reduction is generally performed on a IBM 7090 digital computer according to Vidal's analysis (ref. 22) but transition to a direct reading analog

system, similar to that proposed by Meyer (ref. 23), is now underway. The heat transfer and pressure data are recorded either on dual channel oscilloscopes or on a 28 channel magnetic tape recorder.

The above techniques are used for the quantitative determination of surface heating rates. Another method has been employed in the shock tunnel to determine regions of high heating rates in a qualitative fashion. This consists of painting a model with a low conductivity plastic paint and subjecting to a high temperature shock tunnel flow. The regions of high heat transfer are identified by the formation of scorch patterns. This method has proven useful, for example, in the identification of high heat transfer regions in the vicinity of aerodynamic control surfaces.

Several more or less standard flow visualization techniques are available. These include schlieren, shadowgraph, luminosity, and high-speed motion picture (framing and streak) photography techniques. As can be seen in Fig. 2a, the tunnel has a two axis optical system so that two observations may be made simultaneously when desired.

Another flow visualization technique has been developed which has aided in the interpretation of flow processes occurring about bodies of complicated shapes and in angle-of-attack studies. This involves the observation of surface flow directions through the use of an oil streak technique. Just prior to a test run, thin layers of SAE 30 weight oil mixed with finely divided molybdenum disulfide powder are painted in rings around the models. Apparently, the impulse given to the oil during the short duration test time is of sufficient magnitude both to impart the proper flow direction to the mixture and to thin the layer appreciably so that the streaks are unaffected by the later shock tunnel flow processes (after initial test period). This conclusion has been verified by high speed motion pictures taken during a test run. It was found that the oil streaks begin to form during the high Mach number test flow; however, when long streaks are produced, the latter portions are often a result of the late shock tunnel processes. Thus, only the initial streak directions should be referred to for hypersonic flow information.

Several methods have been investigated for the measurement of model forces and moments in a shock tunnel flow (ref. 22, 24, 25, 26, 27). One that appears to be particularly attractive involves the use of a freely flying lightweight model. In addition to its other advantages it does not require the use of a sting in the test flow, and thus, it eliminates the uncertainties that arise when a sting is present.

Figure 8 is a schematic representation of the method that has been used to obtain lift, drag, and pitching moment data for hypersonic vehicle shapes over an approximate Mach number range of 12 to 24. A lightweight (cast Isofoam, generally from 1 to 5 grams in weight) model is suspended

in the shock tunnel test section on thin (.5 - 1.5 mil diameter) nylon strands. The strands break at the beginning of the test flow, and the model flies freely under the influence of the aerodynamic forces it experiences. For three component studies, the model is flown horizontally, that is, with the force vector in the horizontal plane. A 26,000 frame/second camera (Beckman Whitley Dynaflax) is used to record the model motions. A direct reading of the film upon which a stationary grid is also imaged, provides trajectory information from which force data are deduced.

To minimize the variation of forces during a run, the model center of gravity is adjusted so as to locate it at the center of pressure of the body (actually at a point lying on the line of motion of the resultant aerodynamic force). The c. g. location is obtained by a preferential hollowing out of the model; the pitch moment of inertia is then measured. While models are generally destroyed during test runs, their cost is low, and preparation time is short for most shapes of interest. In practice, the objective of no model rotation, or pitch is difficult to obtain; however, a small amount of rotation can be accepted since its effects on lift, drag and pitching moment can be estimated satisfactorily (ref. 26, 28). It has been found that only a small percentage of the runs made with this technique are not acceptable. Since the model velocity during a typical test period reaches only the order of 1% of the free stream velocity, it is assumed that dynamic effects can be neglected. Figure 9 shows a model in the shock tunnel just prior to a test run.

The following data reduction technique is used to eliminate the need for double differentiation of the model trajectory data. A pitot pressure probe, located in the test section, measures model stagnation pressure during the quasi-steady flow time (see Fig. 8). The free stream dynamic pressure is then calculated from the normal hypersonic relationships, and it is assumed that the q/q_o history is similar to the p_s history. If it is assumed that the force coefficients are constant throughout the run (variations with angle of attack are discussed in reference 26), a trajectory relationship can be established, as shown in Fig. 8. This requires simply a double integration of the q/q_o history. A family of curves for various constant coefficient values (in this case C_L) can be constructed and compared with the observed motion. The best match then gives the actual force coefficient. Figure 10 illustrates the results obtained from this procedure for a typical run on a half cone lifting body.

To our knowledge, personnel of the Naval Ordnance Laboratory, were the first to use freely flying models in shock tunnel flows (refs. 4, 27). The present method, which is suitable for the determination of static aerodynamic co-efficients only, employs an approach different from that used at NOL.

In Fig. 11 are shown shock tunnel performance envelopes upon which are superimposed the conditions at which studies have been made. Also shown are ranges through which it is believed that the present instrumentation can be used, based upon our current experience with these techniques and their ranges of sensitivities.

Present capabilities allow the measurement of static pressures throughout most of the normal driver pressure operating envelope. Surface pressures and heat transfer rates on most configurations can be measured at conditions where viscous interactions have an important effect; while stagnation point properties can be measured down to conditions of free molecule flow. Exact limitations for the determination of forces and moments using the optical tracking technique are difficult to establish, as the amount of model motion obtainable is a function not only of the dynamic pressure but of the model configuration weight, and angle of attack orientation. Stability measurements for axisymmetric ballistic configurations have been made at low angles of attack in the Mach number 12.4 test flow. Forces and moments for lifting bodies, of both simple and complex designs, have been obtained through Mach 23.9.

V. CHARACTERISTICS OF TEST FLOWS

In this section some of the results of studies that have been performed for the purpose of investigating the properties of test section flows will be discussed. In Fig. 12 pitot pressure impact profiles are shown. Figure 12b shows a pitot pressure profile for the complete test section, i.e. to the nozzle walls. When we deduce from this type of data the effective test section area ratio, on the basis of an equilibrium nozzle expansion, the apparent boundary layer displacement thickness is in good agreement with that predicted by Lee (ref. 29). Thus, it is believed that the flow Mach number and other test section properties are well known at least for the conditions at which profiles have been taken and amenable to calculation using the thickness prediction at other points. To give an indication of accuracy, the scatter of the pitot pressure data is approximately $\pm 5\%$ about the mean pitot pressure at the test section for the Mach 12.1 test condition. The scatter in Mach number then is $12.1 \pm .1$.

It has been observed that for various values of the incident shock Mach number in the driven tube, the pressure level in the end of the driven tube - p_5 (or p_{st}) for the reflected nozzle and p_2 for the non-reflected nozzle - exhibits a different time history depending upon the incident shock Mach number. Since this pressure region is essentially the plenum chamber for the test flow in the tunnel nozzle, this behavior will cause a degree of quasi-steadiness in the test section. This is indicated by the shape of the p_{st} (or p_2 in the case of the non-reflected nozzle record). Reflected region pressure records for three different shock Mach number values are shown in Fig. 13. It is believed that a pressure variation in region 5 can be accepted, since flows over models become established quickly in terms of the total test time. Therefore, the true test period is considered to be the time during which the ratio of test section to driver tube pressure is constant. Test section pressures-pitot and static - and their ratios to p_5 in the different regions of shock Mach number operation are also shown in Fig. 13. The indicated flow starting time is the order of 1 millisecond. The constancy of the pressure ratio records is believed to be a reasonably good indication that the variation in test section flow properties can be calculated during the test time based upon the measured p_{st} variation. This also indicates that the boundary layer build-up time is no greater than the apparent flow starting time; in fact, it may be responsible for the apparent starting time.

Operation of a reflected nozzle shock tunnel facility at relatively high stagnation temperatures raises the important question of flow equilibrium during expansion of the test gas to low density levels. Recent works by Nagamatsu, Geiger, and Sheer (ref. 30), Nagamatsu, et al (ref. 31) and unpublished data by Geiger have been employed to construct an approximate

limit above which operation in the thermodynamic and chemical equilibrium regime is indicated. This is shown in Fig. 14 superimposed upon one of the performance envelopes discussed earlier. The data used to construct Fig. 14 were obtained by measuring static pressures along the centerline of an expanding nozzle flow and comparing these results with the calculated equilibrium pressure levels. When the static pressures diverge from the equilibrium values towards an assumed frozen flow model value, the flow is assumed to depart from equilibrium. It has been found that this behavior is almost entirely dependent upon the pressure and temperature levels in the reflected region; that is, it is only a weak function of nozzle area ratio which is in qualitative agreement with the predictions of Bray (32).

Another property of the test section flow which could have an adverse effect on the test data is the flow divergence in the conical nozzle. To investigate this, a force program was conducted using the free flight technique. Here models of varying length but of the same geometry were studied at a constant Reynolds number and Mach number. The configuration was a sphere cone with a 9° half angle. Model length was varied from 1.2 to 6 inches. The results are shown in Fig. 15 for an angle of attack of 22°. Considering the geometry of the models, the Mach number 12.4 test condition, and the angle of the nozzle (15° half angle), one would expect more than a 10% change in the aerodynamic forces as the model length was increased to 6 inches if the divergence pressure change effects were directly reflected in the model surface pressure distributions. However the results in Fig. 15 show that the effects of testing in a divergent flow are not significant for this blunted body. This is probably due to the strong bow shock wave which tends to reduce the pressure drop effect that exists without a model in the flow. The results are in qualitative agreement with the calculations of Henderson and Baradell (33). It is expected that for larger bodies and sharper leading edges, the divergence effects will eventually become important. When studying such shapes, therefore, it will be necessary either to construct parellel flow nozzles or to determine correction factors for the data through the conduction of short studies of the type just discussed.

VI. TYPICAL EXPERIMENTAL RESULTS

In this section typical data obtained in the shock tunnel with the various instrumentation techniques described earlier will be presented to illustrate the types of studies that can be performed. Shown in Fig. 16 is a plot of high Mach number pressure data obtained on a blunted half-cone body over an angle of attack range (ref. 14). These data have pointed out some interesting effects pertaining to the flow around this type of body. For example, the pressure levels on the leeward side are high compared to the free stream pressure while the windward pressures were lower than the Newtonian prediction. The effect of these pressures tend to reduce the lift with respect to the Newtonian prediction in the low angle of attack regimes. These results have been borne out by the results of force and flow visualization studies on the same shape. Heat transfer data for a half-cone body are given in Fig. 17.

Schlieren photographs of representative high Mach number and high temperature model flows are shown in Fig. 18. Also shown is a Schlieren photograph of a Mach 12.1 flow over a half-cone body. Such data while being primarily qualitative, have a quantitative aspect in that it may be used to compare with theoretical predictions when the flow is two dimensional planar or axisymmetric. An experimental shock wave shape is compared to the predicted shape (ref. 16) in Fig. 19, and it is seen that the agreement is good for a significant distance downstream of the nose. Also shown in this figure are pitot pressure data taken through the shock layer and into the free stream several diameters downstream of the nose of the model. Again the agreement with theory is seen to be quite good.

Results from an oil streak surface flow direction study are shown in Fig. 20. The interesting crossflow patterns on the side of a half-cone body can be seen. The flow on the flat surface suggests a tendency for the edges to be trailing edges; however, the streaks turn just before reaching the edges as if diverted by a strong flow over the corner of the model. The presence of a shock wave in this vicinity observed in Schlieren photographs of similar flows, and pressure data also shows that the pressure on these surfaces is significantly higher than expected. Thus, it is felt that the oil streak photographs, when used in conjunction with other data, are valuable in helping to explain the phenomena that occur in flows over complicated shapes such as the one shown here.

In Fig. 21 is shown a summary of force and moment data obtained on a half-cone lifting body (ref. 28). The shapes of the force coefficient curves obtained are in agreement with a simplified Newtonian prediction.

Figure 22 is a photograph of experimental equipment tested recently in the shock tunnel. This study has the objective of determining the magnitude and predictability of magnetohydrodynamic control forces generated in

an entry vehicle flow field. A 15,000 gauss magnetic field is applied normal to the flow in the channel between the electrode wedges. Pressure distributions on the surface through the channel are measured as well as the drag force on the complete model. The channel flow may be seeded by injection of material into the flow field at the nose of the model. Various cathode materials are being studied, and there is an independent cathode heating circuit which brings it to its emission threshold temperature. The resistance in the electrode circuit can be varied from run to run so that MHD power curves can be determined as functions of the variables under investigation. Supporting this study, a technique has been developed to measure the effective conductivity of the flow through the channel. Some of the results of this work have been reported in reference 20.

VII. CONCLUDING REMARKS

The shock tunnel can produce flows of air of good quality over wide ranges of Mach number, Reynolds number, and stagnation temperature (enthalpy), and that instrumentation techniques are available which allow the measurement of many important aerodynamic properties.

Several aerodynamic problem areas of interest in the current atmospheric entry technology have been discussed on a broad basis, and it is concluded that the simulation capabilities of the shock tunnel are compatible with the simulation requirements of these problems over reasonably wide ranges of variables. The shock tunnel is, of course, restricted to the study of problems that do not require long-time simulation.

On the basis of available data, the problem of nozzle flow non-equilibrium is not encountered for certain ranges of tunnel operation. However, for other ranges non-equilibrium effects exist and their influence on test results must be further investigated. To reduce the regions of uncertainty with a reflected nozzle shock tunnel, operation at high reflected region pressures is called for, as suggested in references 1 and 31. In addition to determining the effects of non-equilibrium free stream flows on test results, the shock tunnel is well suited, first, for the direct study of the controlled expansion of a reacting gases in the nozzle and, second, for the study of the aerodynamic effects of non-equilibrium in the flow about bodies.

Current limitations on shock tunnel performance concern, first, its instrumentation capabilities and, second, its ability to provide simulation of flow conditions that will be encountered by vehicles entering the atmosphere at velocities significantly greater than satellite velocity (see Fig. 4). In the former case, development of existing techniques should be continued for the purpose of increasing their accuracy and sensitivity, and new techniques, primarily those concerned with the determination of gaseous and plasma properties (ref. 20) should be developed. For the purpose of improving their performance characteristics, test section size can be increased significantly without employing an unreasonably large shock tube section (ref. 34). This would allow large scale simulation when required (1); however it appears that progress is required primarily in the development of high temperature, high pressure driver techniques. Examples of work toward this end are discussed in references 34, 35, and 36.

NOMENCLATURE

A	area
C_D	drag coefficient
C_L	lift coefficient
C_{MR}	2nd moment coefficient
D	drag
h	enthalpy
L	lift, body length
M	Mach number
M_S	shock Mach number
p	pressure
q	dynamic pressure
q	heat transfer rate
R	base radius
Re	Reynolds number
r	local radius
T	temperature
t	time
U	velocity
X	drag coordinate
x	body coordinate
Y	lift coordinate
α	angle of attack

γ	ratio of specific heats
N_e	electron density
N_K	Knudsen number
λ	mean free path
γ_E	entry angle
ρ	density
Θ_c	cone half angle
$\bar{x}$	$M_\infty^3 \Big/ \sqrt{Re_\infty / IN}$

SUBSCRIPTS

c.g.	center of gravity
c.p.	center of pressure
n	nose
p	pitot
s	stagnation
2	behind driven tube incident shock wave
1	initial driven tube
5, st	reflected region or reservoir
w	wall
∞	free stream

REFERENCES

1. Hertzberg, A. and Wittliff, C. E. , ; Studying Hypersonic Flight in the Shock Tunnel; IAS paper No 60-67 Presented at the IAS National Summer Meeting, Los Angles, California, June 28-July 1, 1960.

2. Yoler Y. A. ; Hypersonic Shock Tube; GALCIT Memo No. 18;July, 1954.

3. Nagamatsu, H. T. , Geiger, R. E. and Sheer, R. E. Jr. ; Hypersonic Shock Tunnel; ARS Journal, Vol. 29, M ay, 1959.

4. Aronson, P. M. , Marshall T. , Seigel, A. E. , Slawsky, Z. I. , and Smiley, E. F. ; Shock Tube Wind Tunnel Research at the U. S. Naval Ordnance Laboratory AFSWC Proceedings of 2nd Shock Tube Symposium; SWR-TM-58-3, March, 1958.

5. Warren, W. R. ; The Design and Performance of the General Electric Six Inch Shock Tunnel; AFSWC Proceedings of 1st Shock Tube Symposium; SWR-TM-57-2, February, 1957.

6. Kaegi, E. M. , Warren, W. R. ; Vitale, A. J. ; Experimentation with the General Electric Six Inch Shock Tunnel; AFSWC Proceedings of 2nd Shock Tube Symposium; SWR-TM-58-3, March, 1958.

7. Warren, W. R. ; Laboratory Experimental Studies in Re-Entry Aerothermodynamics; Proceedings of the 10th International Astrounautical Congress; London, 1959.

8. Wittliff, C. E. , Wilson, M. R. and Hertzberg, A. ; The Tailored-Interfaced Hypersonic Shock Tunnel; ASME-ARS Aviation Conference, Dallas, Texas, March, 1958; J. Aero/Space Sci. Vol. 26, No. 4, April, 1959.

9. Glick, H. S. , Hertzberg, A. , and Smith W. E. ; Flow Phenomena in Starting a Hypersonic Shock Tunnel; CAL Rept. No. AS-789-A-3; AEDC-TN-55-16; March, 1955.

10. Kaegi, E. M. and Warren, W. R. ; The Free Stream Properties of Argon Free Air in Chemical Equilibrium for a One Dimensional Isentropic Expansion Process, General Electric TIS R61SD111, Dec. 1961.

11. Scala, S. M. ; Hypersonic Viscous Shock Layer; ARS Journal Vol. 29, No. 7 pp. 520-522; July, 1950.

12. Erickson, W. D. and Creekmore, H. S. ; A Study of Equilibrium Real Gas Effects in Hypersonic Air Nozzles, Including Charts of Thermodynamic Properties for Equilibrium Air; NASA TN-D-231; April 1960.

13. Thomas, R.E. and Lee, J.D.; The Ohio State University 12 Inch Hypersonic Wind Tunnel System; WADC TN-59-280; July 1959.

14. Engel, M.J., Geiger, R.E., Harris, C.J., Kaegi, E.M., and Warren, W.R.; Aerodynamic Force Heat Transfer and Pressure Measurements on a Lifting Body Configuration at Mach Number 17; General Electric MSVD Final Report. BAC 2-876316-7663; April, 1960.

15. Galman, B.A.; Direct Re-Entry at Escape Velocity; G.E. TIS R60SD357; April, 1960.

16. Gravalos, F.G., Edelfelt, I.H. Emmons, H.W.; The Supersonic Flow About a Blunt Body of Revolution for Gases at Chemical Equilibrium, G.E. TIS R58SD245; June 1958.

17. Eschenroder A.Q., and Daiber, J.W.; Ionization Nonequilibrium in Expanding Flows; ARS Preprint 1458-60; Presented at the ARS 15th Annual Meeting, Washington, D.C.; December, 1960.

18. Eschenroder A.Q., and Daiber, J.W., Golian, T.C., and Hertzberg, A.; Shock Tunnel Studies of High-Enthalpy Ionized Air Flows; CAL.; Presented at the ARGARD Meeting on High Temperature Aspects of Hypersonic Fluid Dynamics; Brussels, Belgium; March, 1962.

19. Hall, G.J., Eschenroder, A.Q., and Marrone, P.V.; Inviscid Hypersonic Air-Flow with Coupled Nonequilibrium Processes; IAS Paper No. 62-67 Presented at the I.A.S. 30th Annual Meeting New York, N.Y.; January, 1962.

20. Muntz, E.P., Harris, C.J., and Kaegi, E.M.; Techniques for the Experimental Investigation of the Properties of Electrical Conducting, Hypersonic Flow Fields; Presented at the Second National Symposium on Hypervelocity Techniques; Univ. of Denver; Denver, Colorado; March, 1962.

21. Harris, C.J. and Kaegi, E.M.; The Application of Pressure and Force Transducers in Shock Tunnel Aerodynamic Studies; G.E. TIS R59SD327; also presented at AFSWC 3rd Shock Tube Symposium, March, 1959.

22. Vidal, R.J.; Model Instrumentation Techniques for Heat Transfer and Force Measurements in a Hypersonic Shock Tunnel; CAL Rept. No. AD-917-A-10;WADC TN 56-315; February, 1956.

23 Meyer, R.F.; A Heat-Flux Meter for Use with Thin Film Surface Thermometers; National Research Council of Canada; Aero. Report LR-279; April, 1960.

24. Wittliff, C.G. and Rudinger, G.; Summary of Instrumentation Development and Aerodynamic Research in a Hypersonic Shock Tunnel; WADC TR 58-401, August, 1958.

25. Martin, J.F., Durea, G.R., and Stevensen, L.M.; Instrumentation for Force and Pressure Measurements in a Hypersonic Shock Tunnel; Presented at the Second Symposium on Hypervelocity Techniques; Univ. of Denver, Denver, Colorado; March,. 1962.

26. Kaegi, E.M., Malczynski, J.R. and Warren, W.R.; The Measurement of Aerodynamic Forces in Shock Tunnel Test Flows; G.E. TIS R60SD339, April, 1960.

27. Seigel, A.E.; Millisecond Measurement of Forces and Moments in Hypersonic Flow; Addresses at the Dedication of the new Aeroballistic Research Facilities and at the Decennial Symposium on Aeroballistics, NOLR 1238; White Oak Silver Spring, Md., May 25-26, 1959.

28. Geiger, R.E.; Experimental Lift and Drag of a Series of Glide Configurations at Mach Numbers 12.6 and 17.5; Jour. of the Aerospace Science; Vol 29, No. 4 pp. 410-419; April, 1962.

29. Lee, J.D.; Axisymmetric Nozzles for Hypersonic Flows; Report TN (ALSOSU)-459-1; Ohio State University Research Foundation; July, 1959.

30. Nagamatsu, H.T., Geiger, R.E., Sheer, R.E.; Real Gas Effects in Flow over Blunt Bodies at Hypersonic Speeds; JA SS, Vol. 27, No. 4; April, 1960.

31. Nagamatsu, H.T., Workman, J.B. and Sheer, R.E.; Hypersonic Nozzle Expansion wiyh Air Atom Recombination Present. Journal Aero. Space Science Vol 28, No. 11 pp. 833-837, November, 1961.

32. Bray, K.N.C.;Atomic Recombination in a Hypersonic Wind Tunnel Nozzle; J. Fluid Mech, Vol. 6, Pt 1, pp 1-32; July, 1959.

33. Henderson, A., Jr. and Baradell, D.L.; Recent Work at Langley Research Center in the Development of Hypersonic Helium Tunnels; Proceedings of Hypervelocity Techniques Symposium, Denver, Colorado, Oct. 20-21, 1960.

34. Hilton, J., Fabian, G., Golian, T., Wilson, M., and Somers, L., Development and Performance of the C.A.L. Six Foot Shock Tunnel; Presented at the Second Symposium on Hypervelocity Techniques; Univ. of Denver; Denver, Colorado; March, 1962.

35. Warren, W.R., Rogers, D.A. and Harris, C.J.; The Development of an Electrically Heated Shock Driven Test Facility; Presented at the Second Symposium on Hypervelocity Techniques; Univ. of Denver, Denver, Colo.; March, 1962.

36. Camm, J.C.; Escape Velocity Shock Tube with Arc Heated Driver; Presented at the Second Symposium on Hypervelocity Techniques; Univ. of Denver, Denver, Colo.; March, 1962.

TABLE 1

CLASSIFICATION OF SEVERAL AERODYNAMIC

PROBLEM AREAS IN ATMOSPHERIC ENTRY STUDIES

Problem Area	Simulation Considerations
Lifting Vehicle Aerodynamic Characteristics Forces and Moments Heat transfer Problems	Wide M and Re ranges, wide $\bar{x}$ range, Moderate T_s (Tw/Ts) range.
Ballistic Vehicle Aerodynamic Characteristics	Same
Hypersonic Flow Studies Inviscid Flows Interaction Effects Separated Flows	Same, but add wider T_s range
Low Density Aerodynamics Strong Interaction (Merged) Slip Effects	Wide M range, high $\bar{x}$ (and N_k) range, wide T_s range
Magnetohydrodynamics Force Generation Heat Transfer Modification	High T_s range, wide Re range, wide N_e range (seeding possible), M simulation relaxed.
Plasma-Microwave Interactions	Same

TABLE 2

MODEL INSTRUMENTATION TECHNIQUES

Technique	Description
Pressure Distribution Measurement	Piezoelectric crystal gages, recessed and shock mounted, dynamically and statically calibrated.
Heat Transfer Distribution Measurement	
Quantitative	Sputtered platinum thin film resistance thermometers. Thick film resistance thermometers (calorimeter gages).
Qualitative	Scorch patterns on surfaces of low thermal conductivity.
Flow Visualization	Schlieren and shadowgraph spark photography, luminosity photography, high speed framing cameras, 2 axis optical system.
Surface Flow Direction Observation	Oil streak patterns established by test flow.
Aerodynamic Forces and Moments	Freely flying, lightweight models tracked by high speed framing camera. Three component static data obtained (6 components feasible).

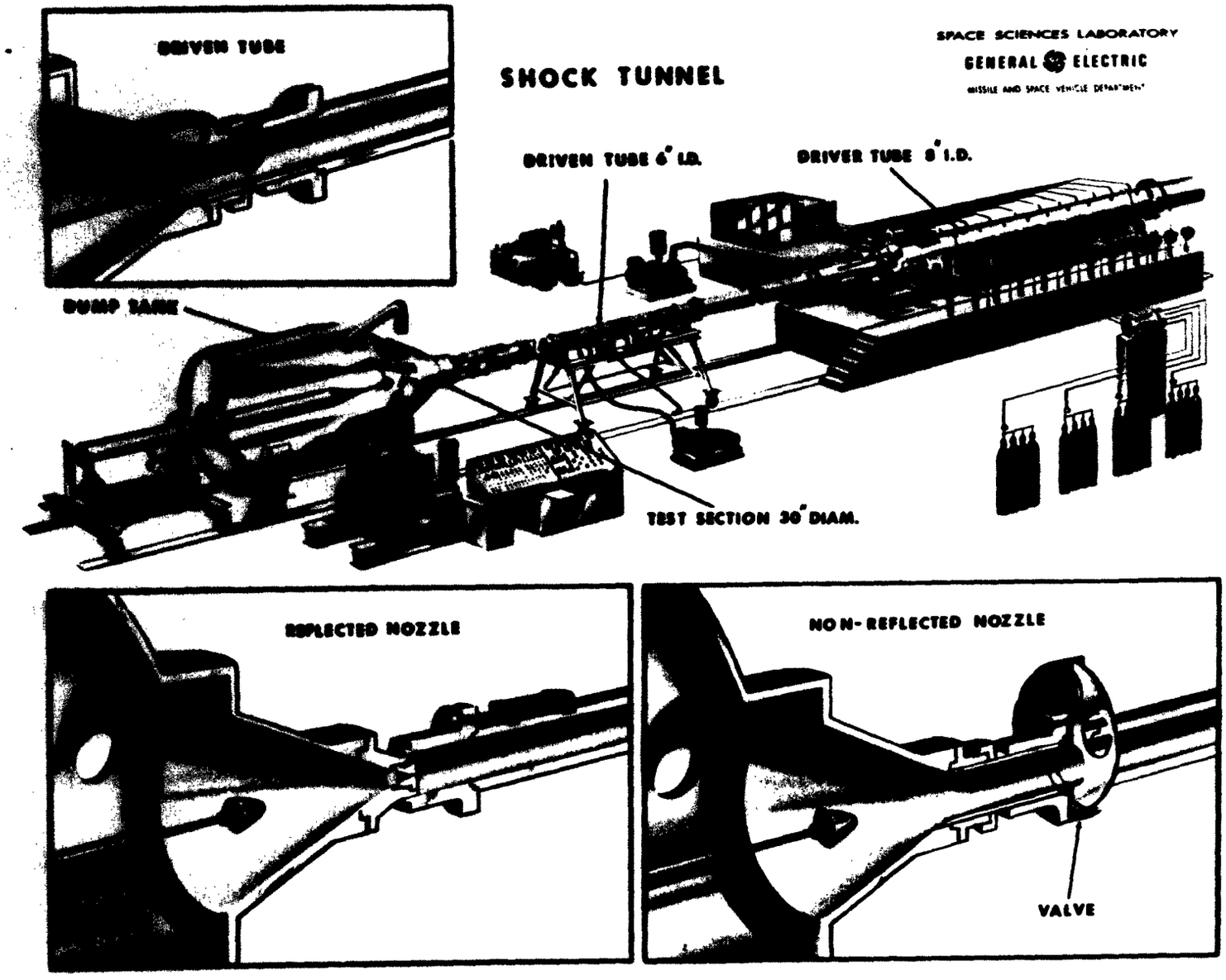

Figure 1. Thirty-inch Shock Tunnel

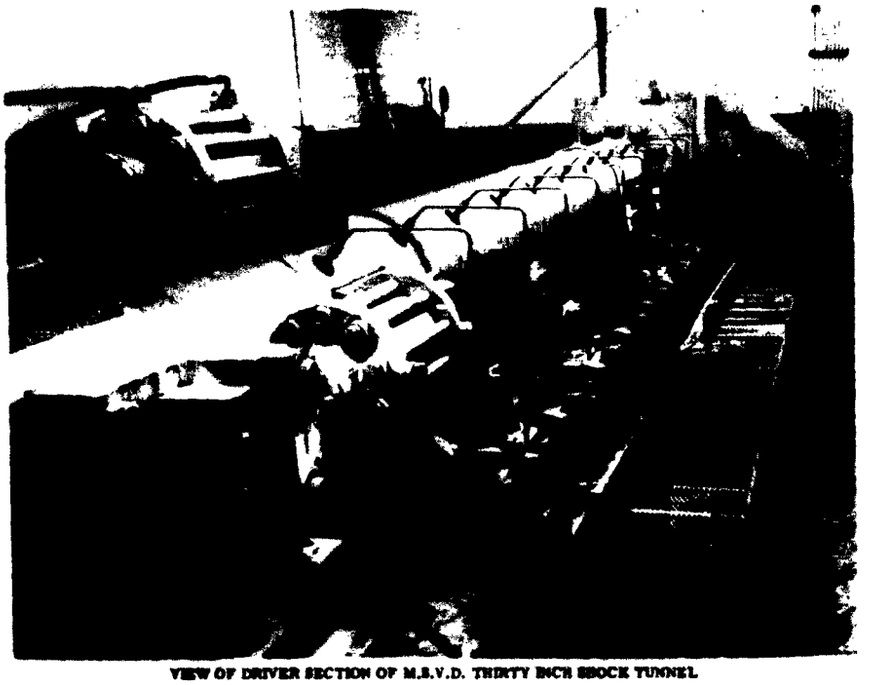

VIEW OF DRIVER SECTION OF M.S.V.D. THIRTY INCH SHOCK TUNNEL

Figure 2a.

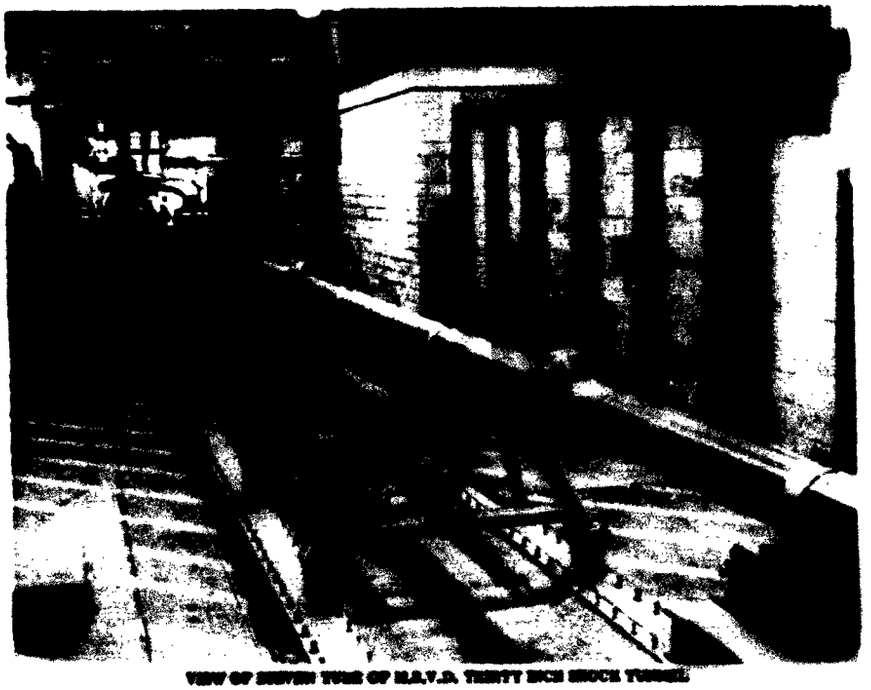

VIEW OF SHOCK TUBE OF M.S.V.D. THIRTY INCH SHOCK TUNNEL

Figure 2b.

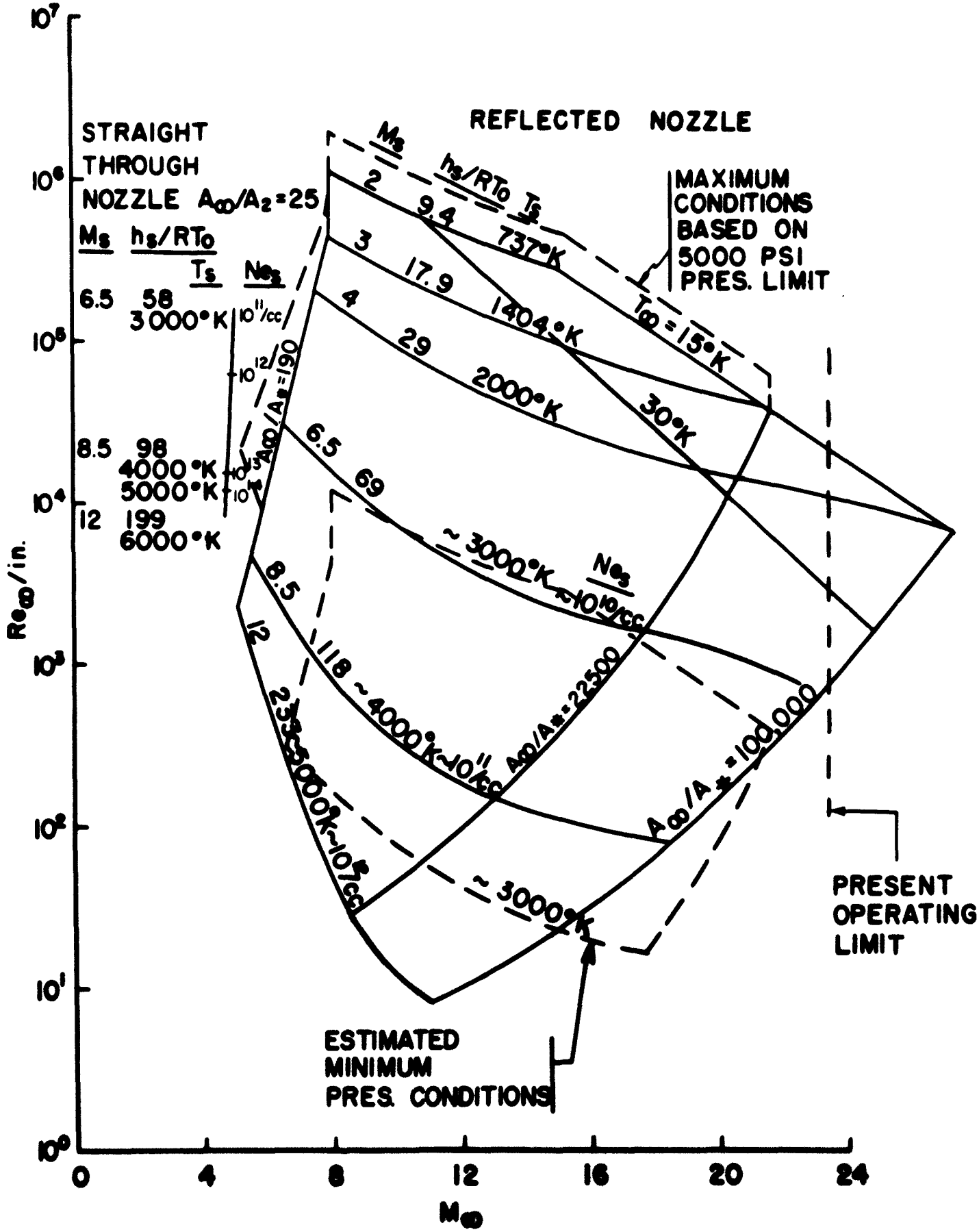

Figure 3a. Performance Envelope for MSVD Shock Tunnel

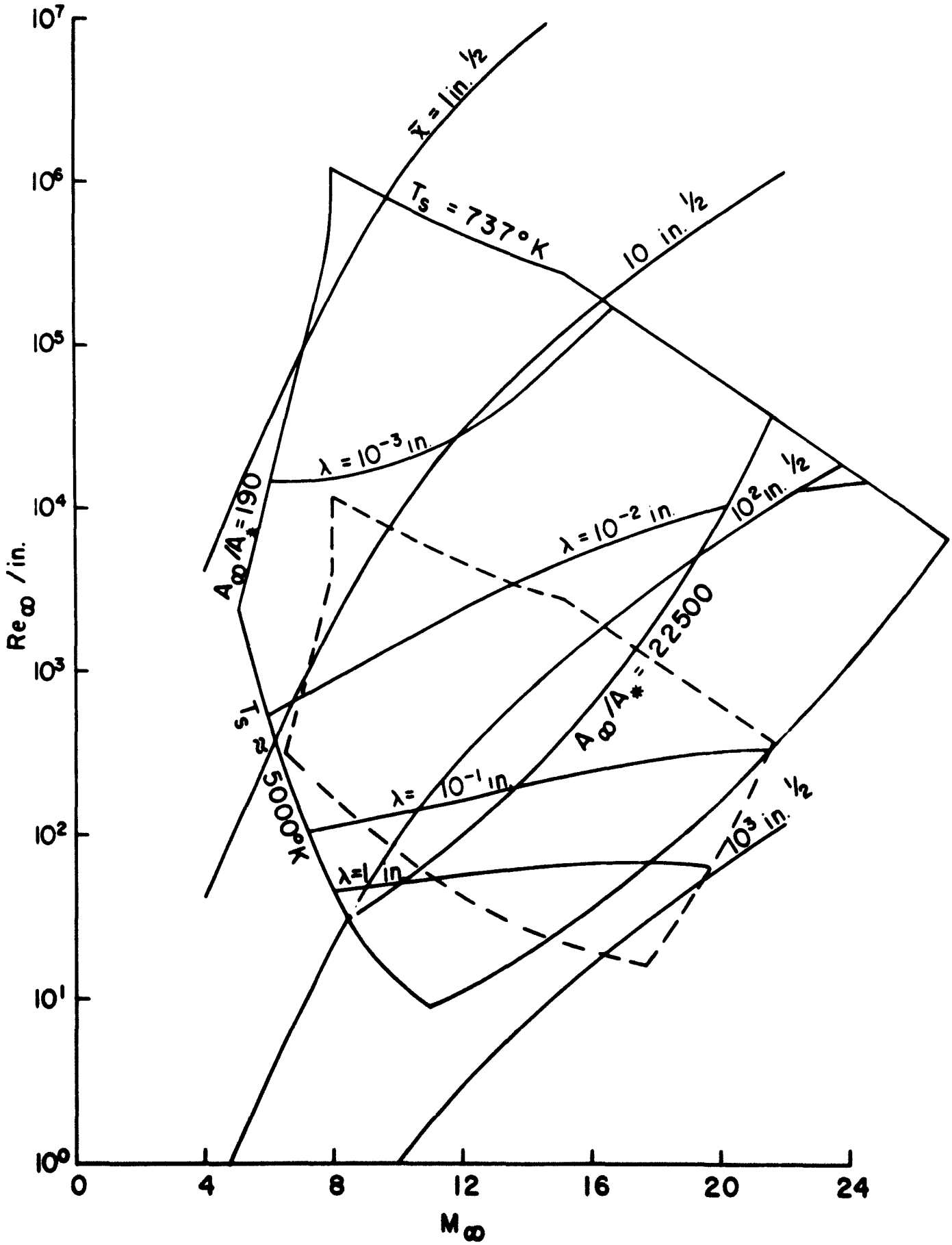

Figure 3b. λ and $\bar{\chi}$ For Reflected Nozzle Performance Envelope

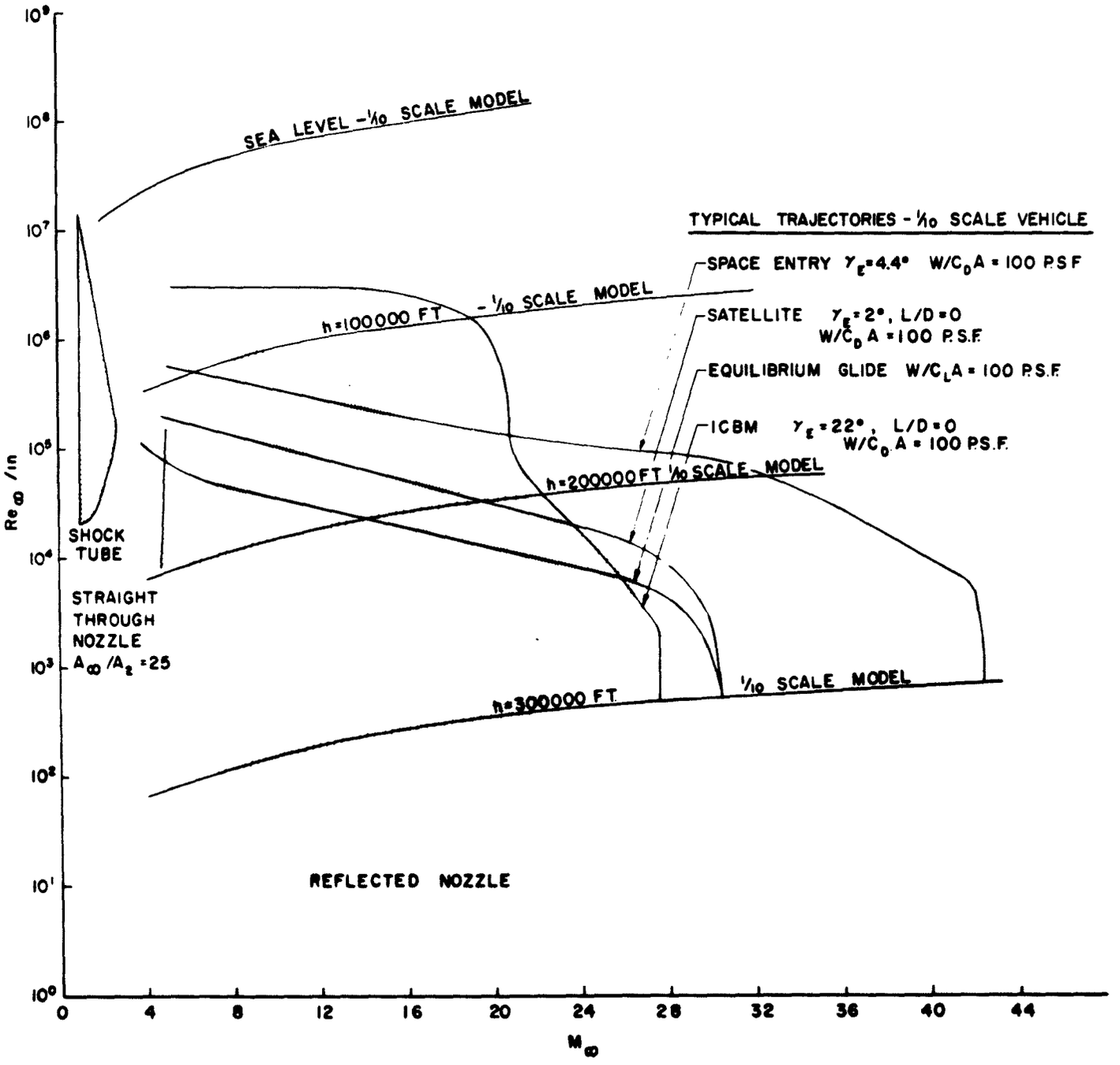

Figure 4. Typical Entry Trajectories Compared to Shock Tunnel Performance Envelope

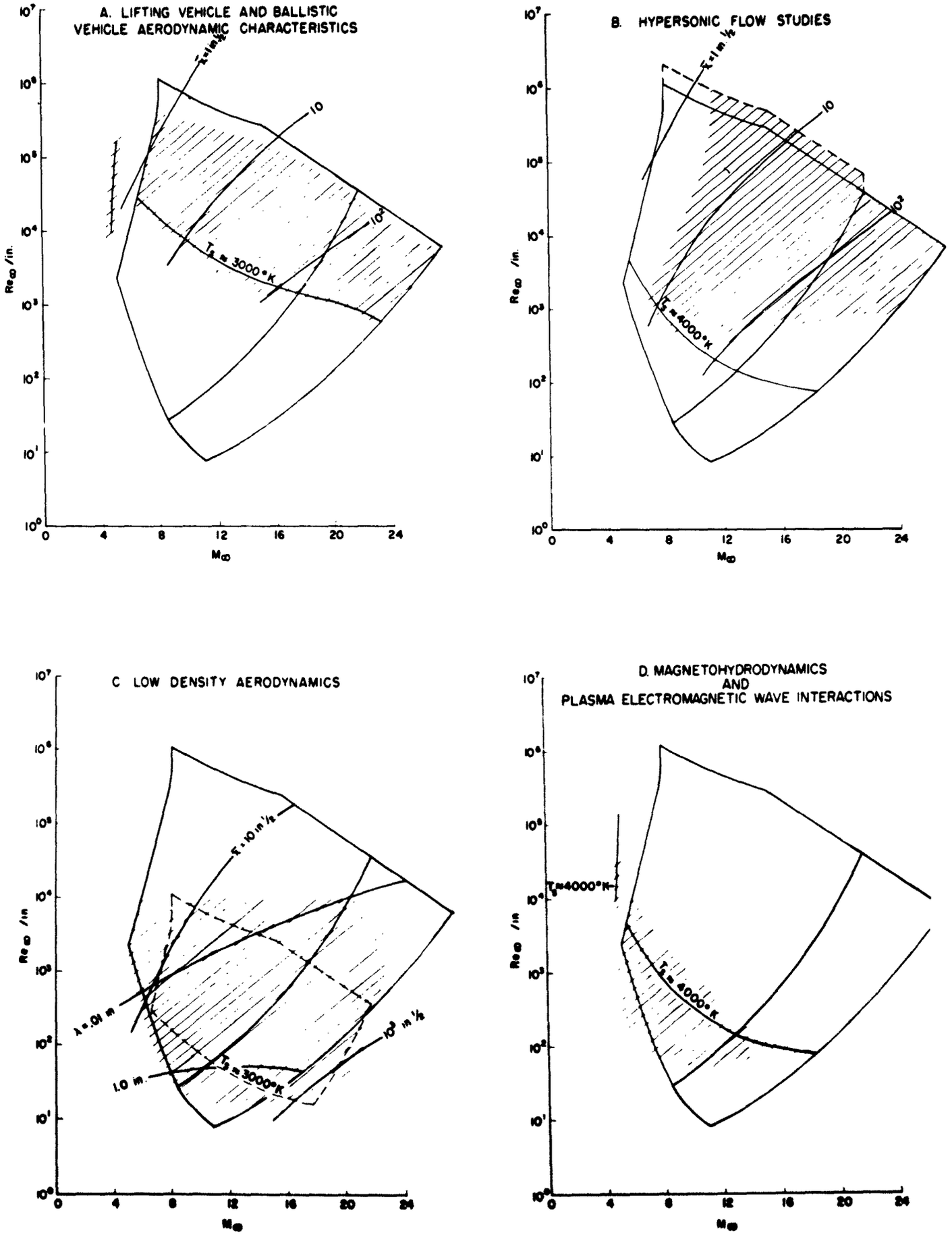

Figure 5. Problem Study Regions

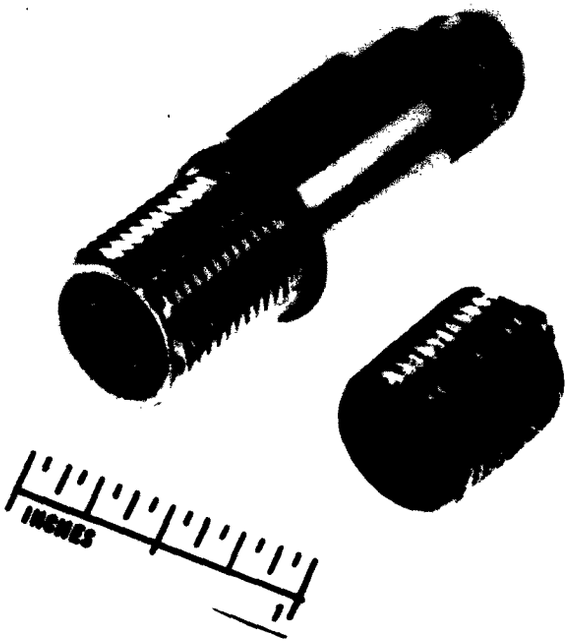

QUARTZ AND BARIUM TITANATE CRYSTAL PIEZOELECTRIC TRANSDUCERS

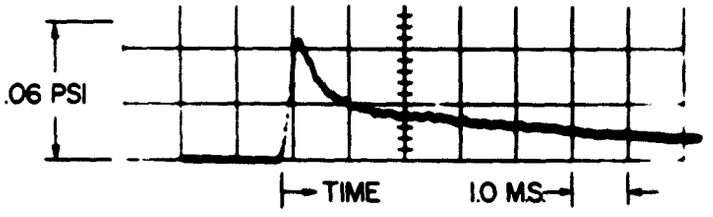

BARIUM TITANATE CRYSTAL PRESSURE GAGE RESPONSE

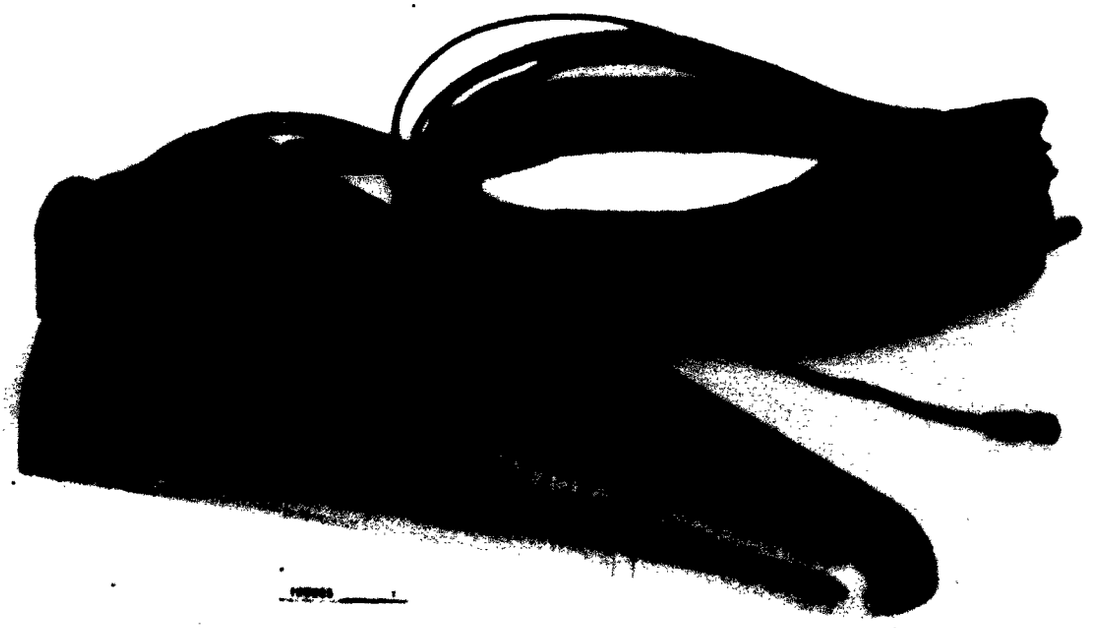

SHOCK TUNNEL PRESSURE MODEL OF A HALF SPHERE CONE BODY

Figure 6.

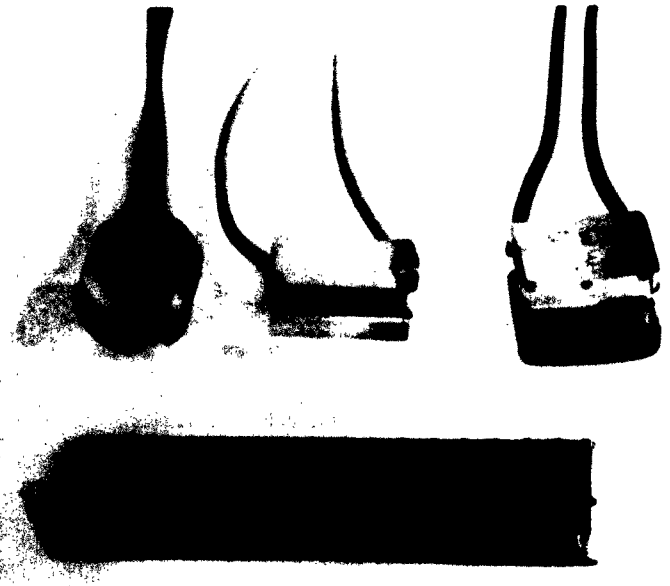

THIN FILM RESISTANCE THERMOMETERS MOUNTED ON VARIOUSLY CONTOURED QUARTZ PLUGS

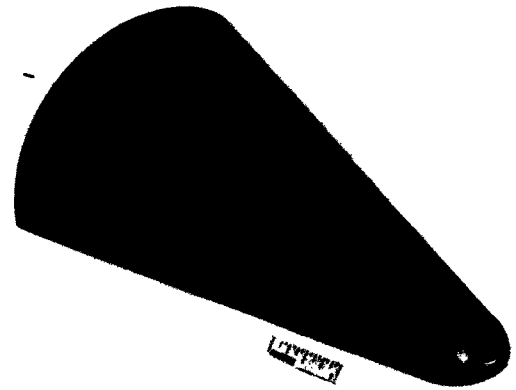

SHOCK TUNNEL HEAT TRANSFER MODEL OF A HALF SPHERE CONE BODY

RESISTANCE THERMOMETER TEMPERATURE RESPONSE AND HEAT TRANSFER RATE HISTORY

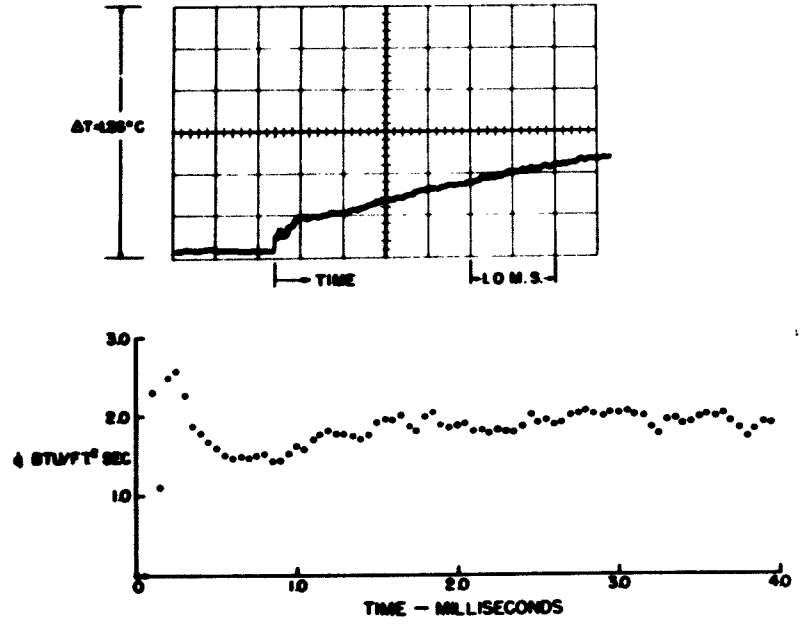

Figure 7.

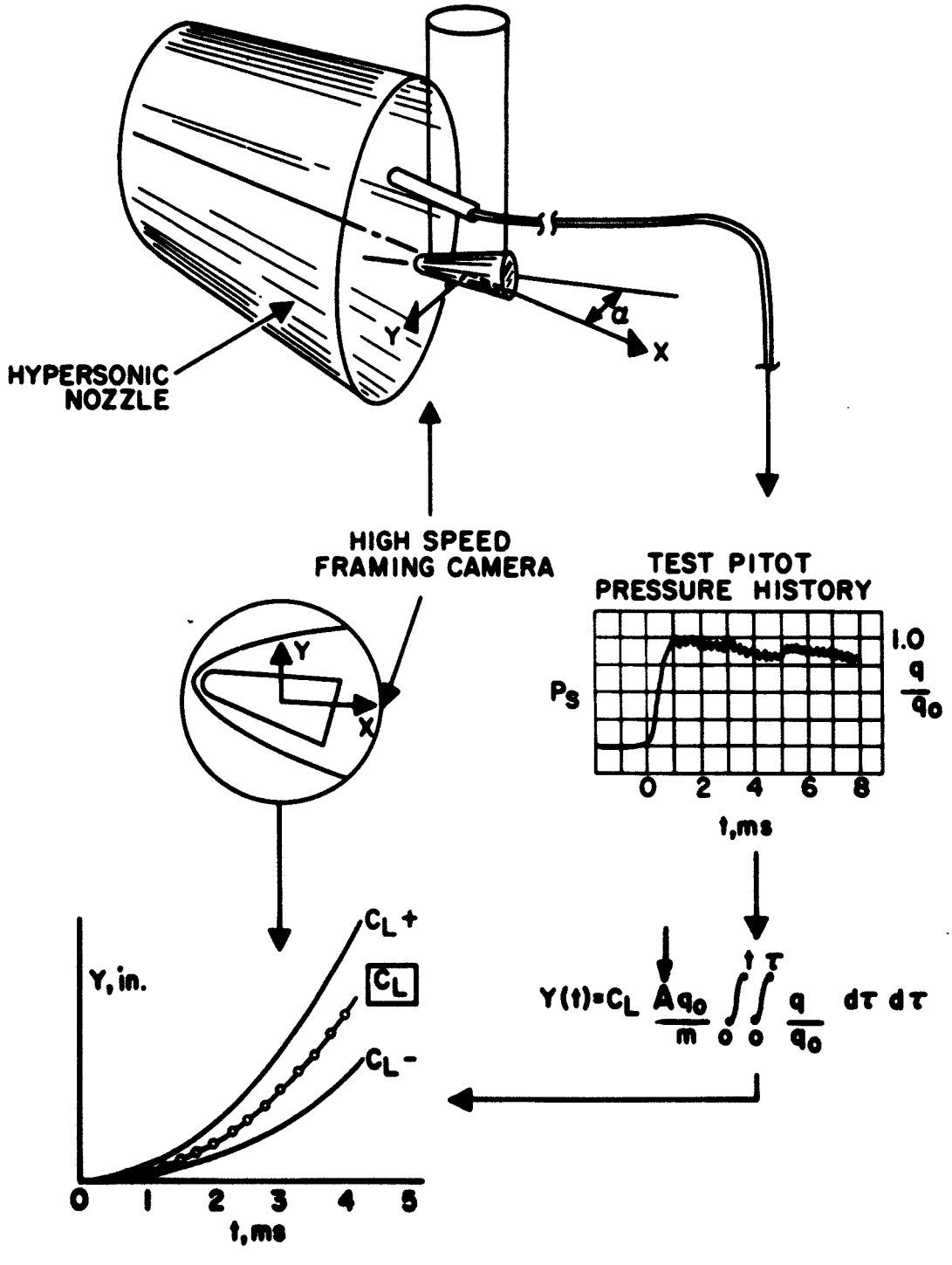

Figure 8. Free Flight Force Measurement

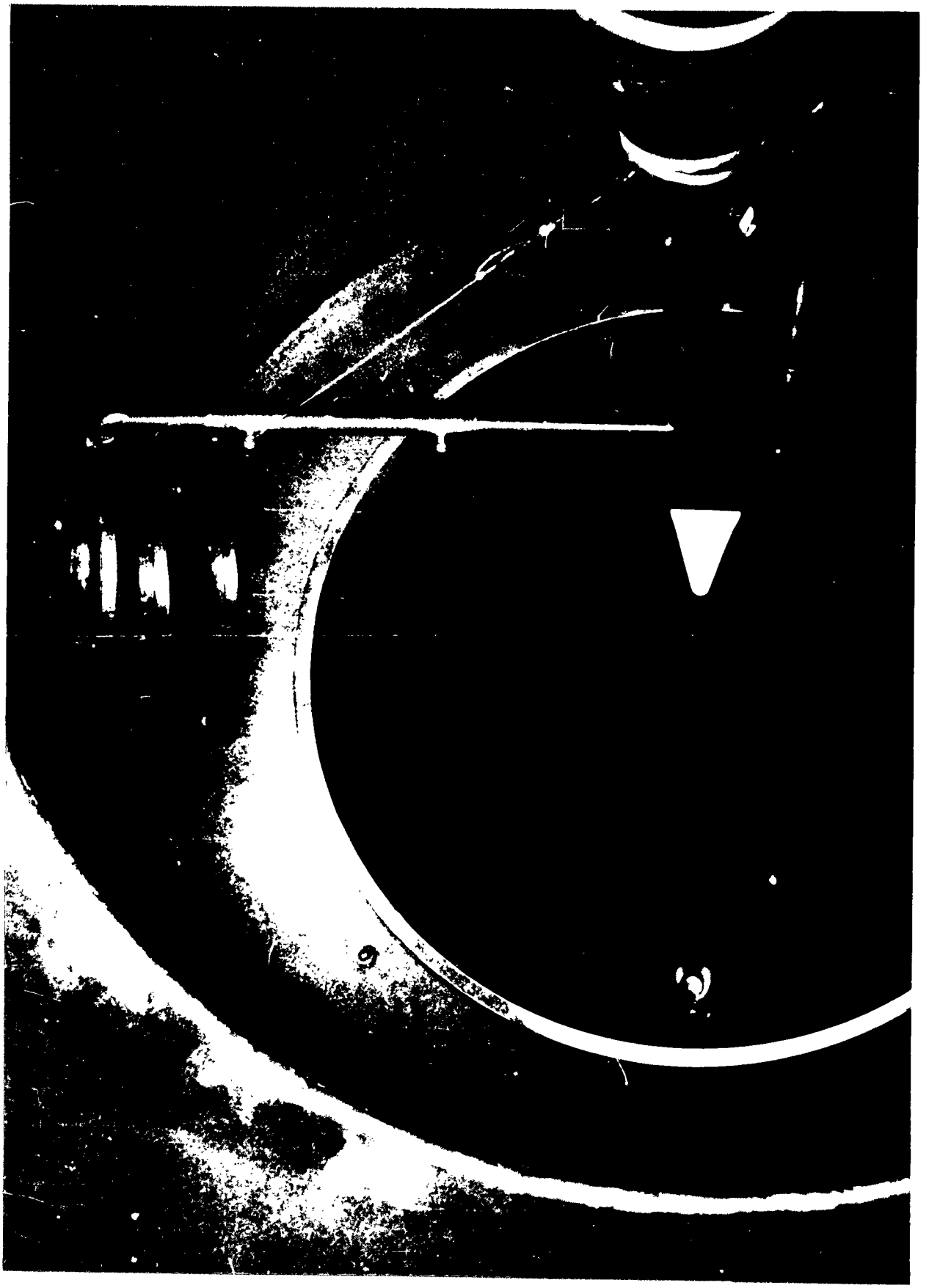

Figure 9. Free Flight Model Suspended in the Shock Tunnel

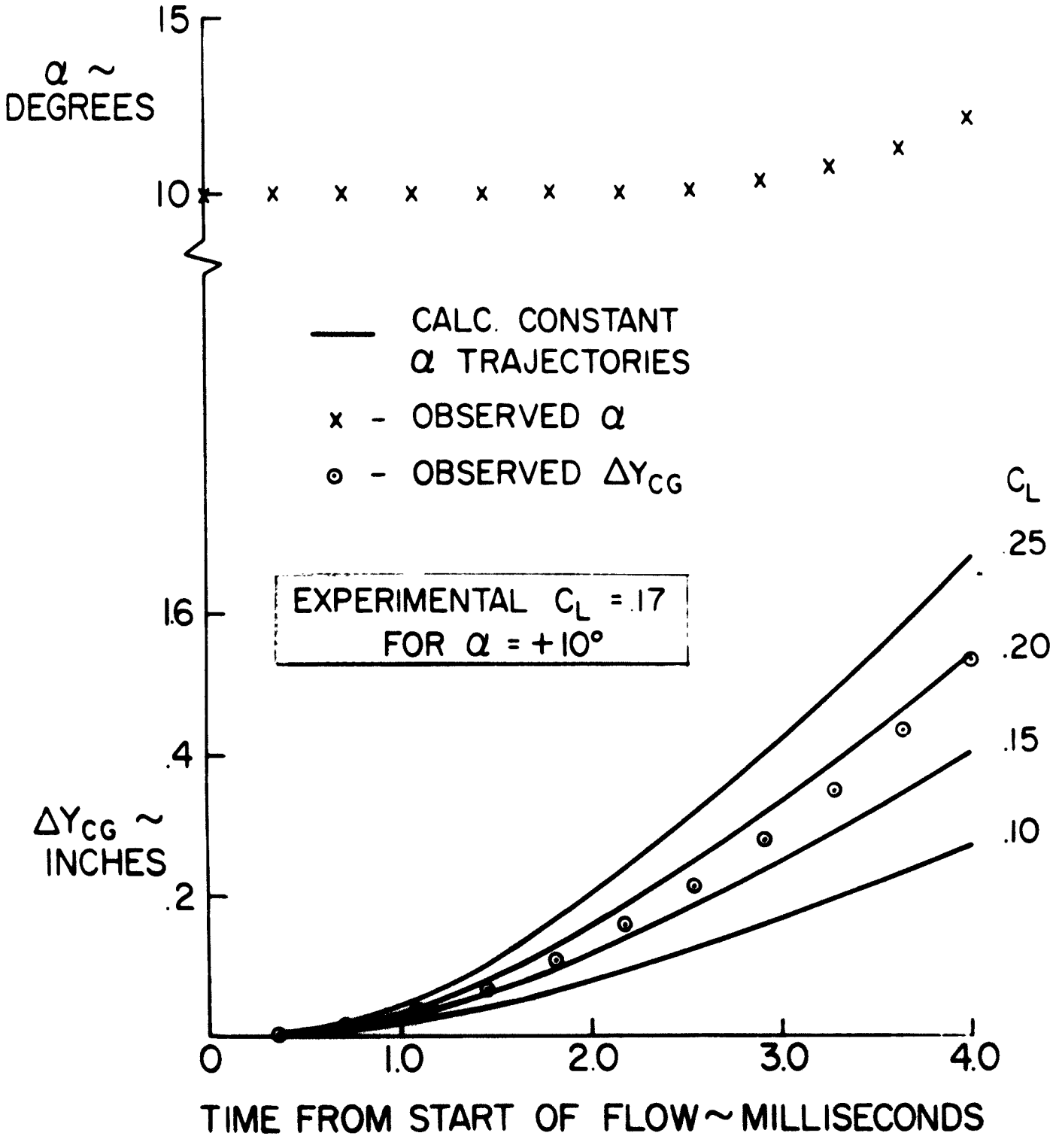

Figure 10. Trajectory Matching Scheme for Lift (And Drag) Coefficient Determination

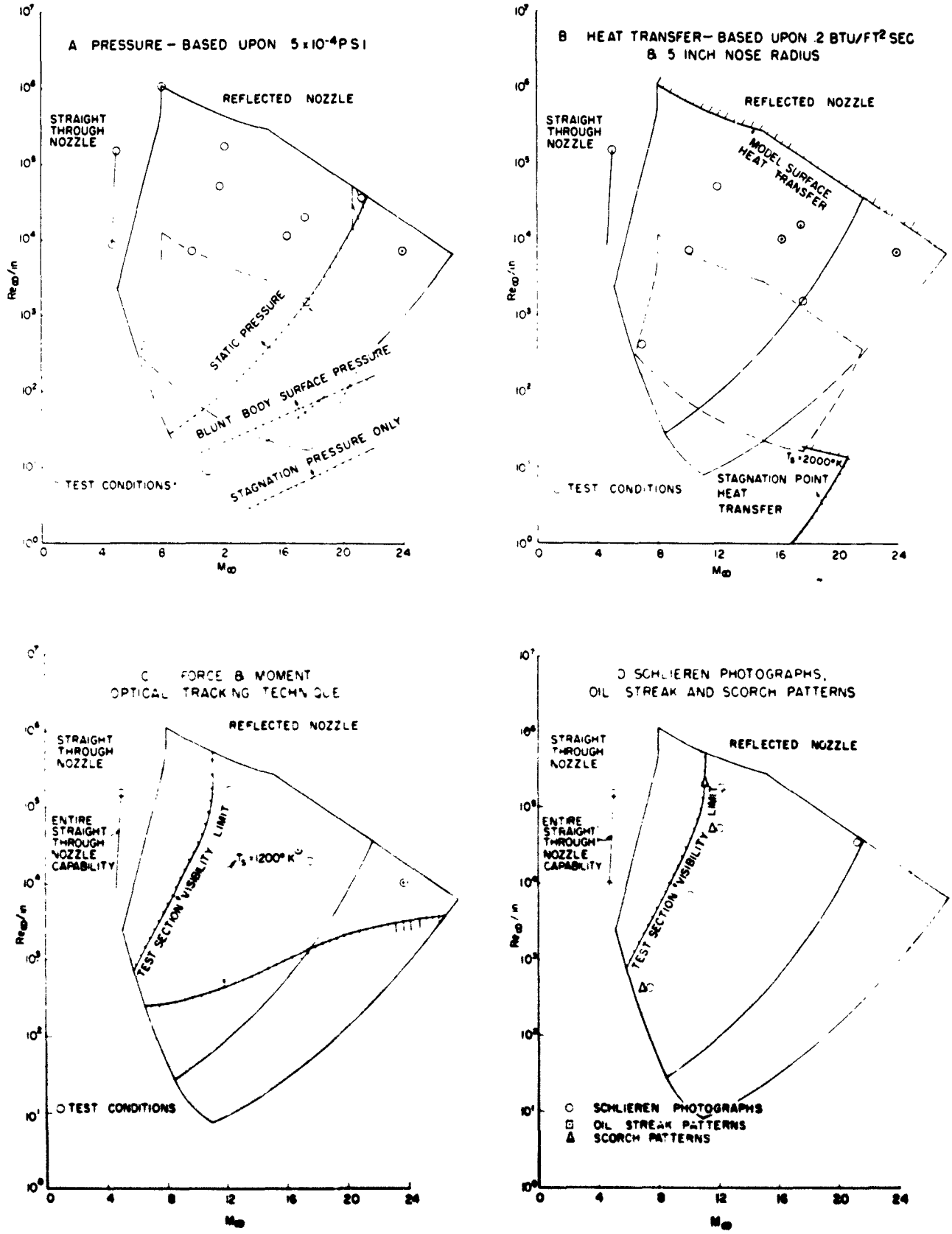

Figure 11. Instrumentation Sensitivity Limits

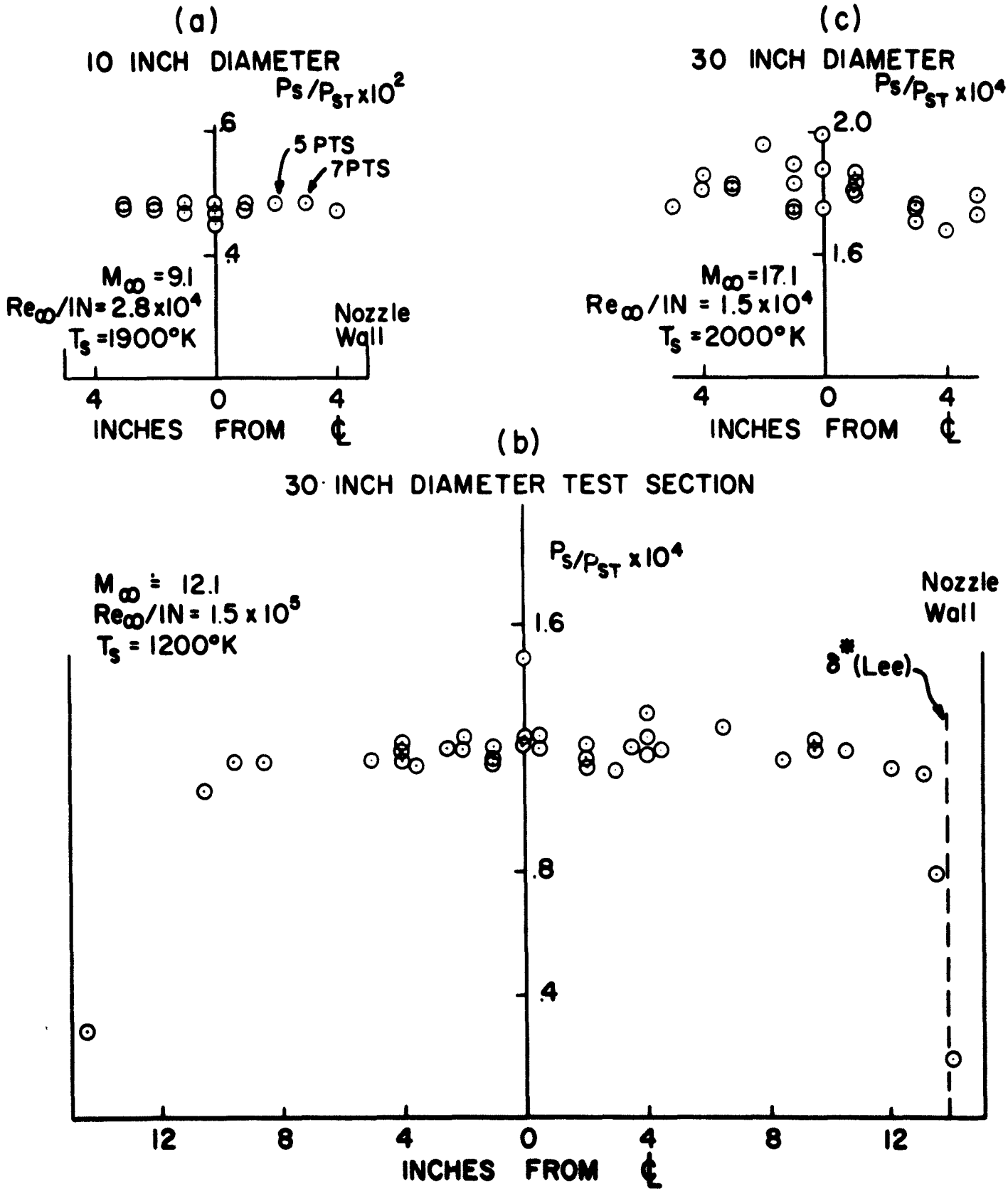

Figure 12. Shock Tunnel Impact Surveys

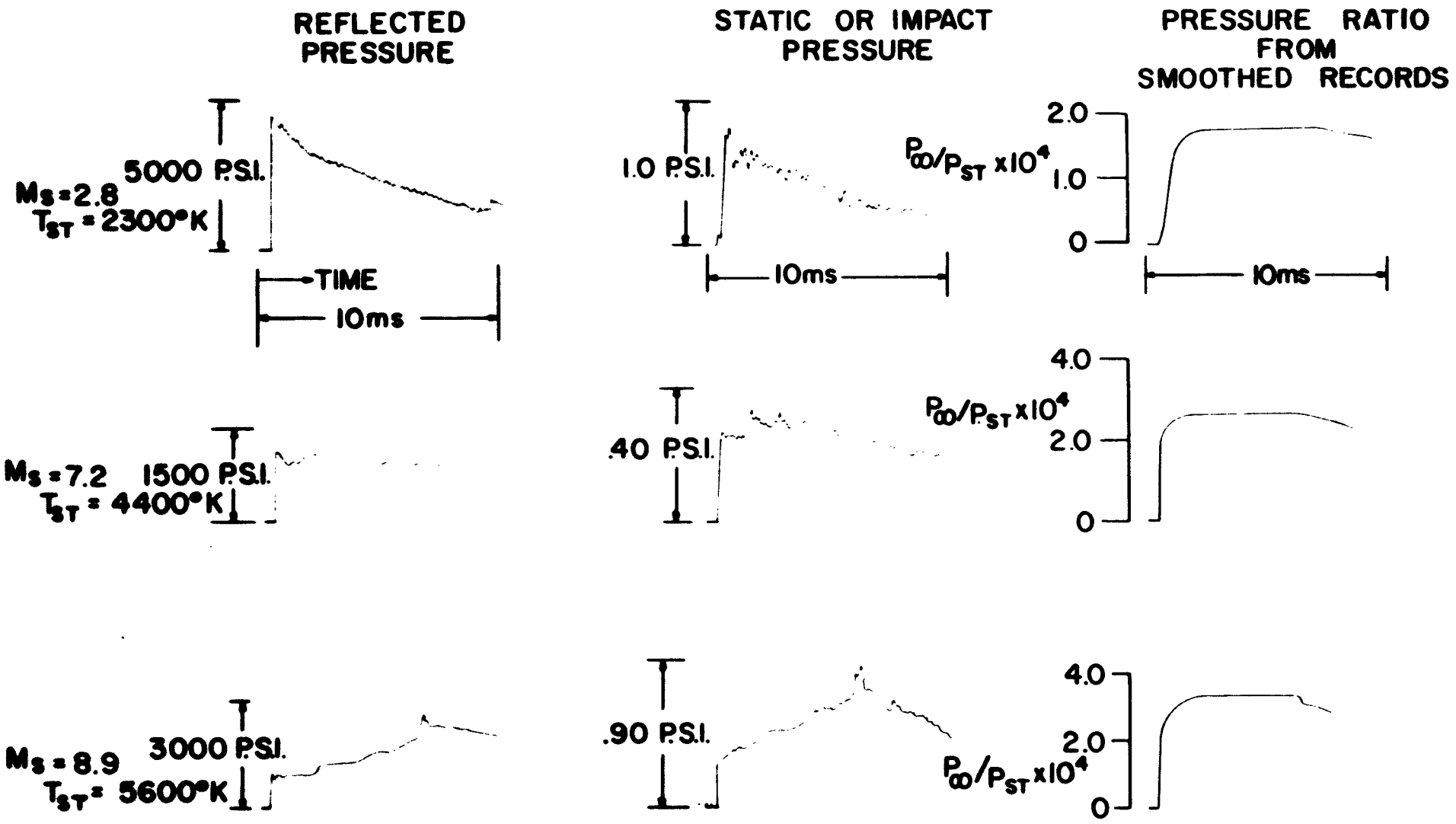

Figure 13. Studies of Pressure Ratio Steadiness

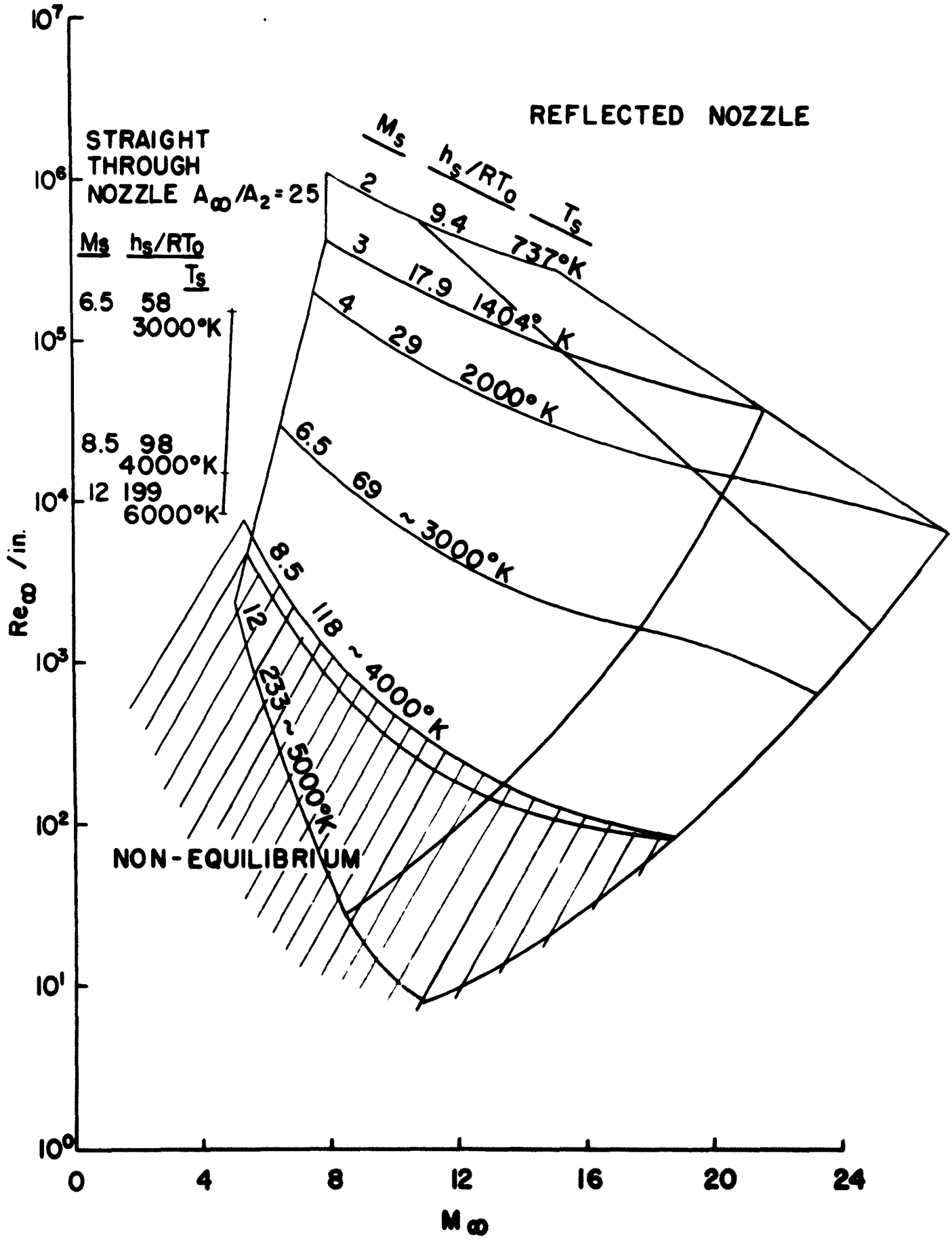

Figure 14. Region of Flow in Chemical Equilibrium for MSVD Shock Tunnel

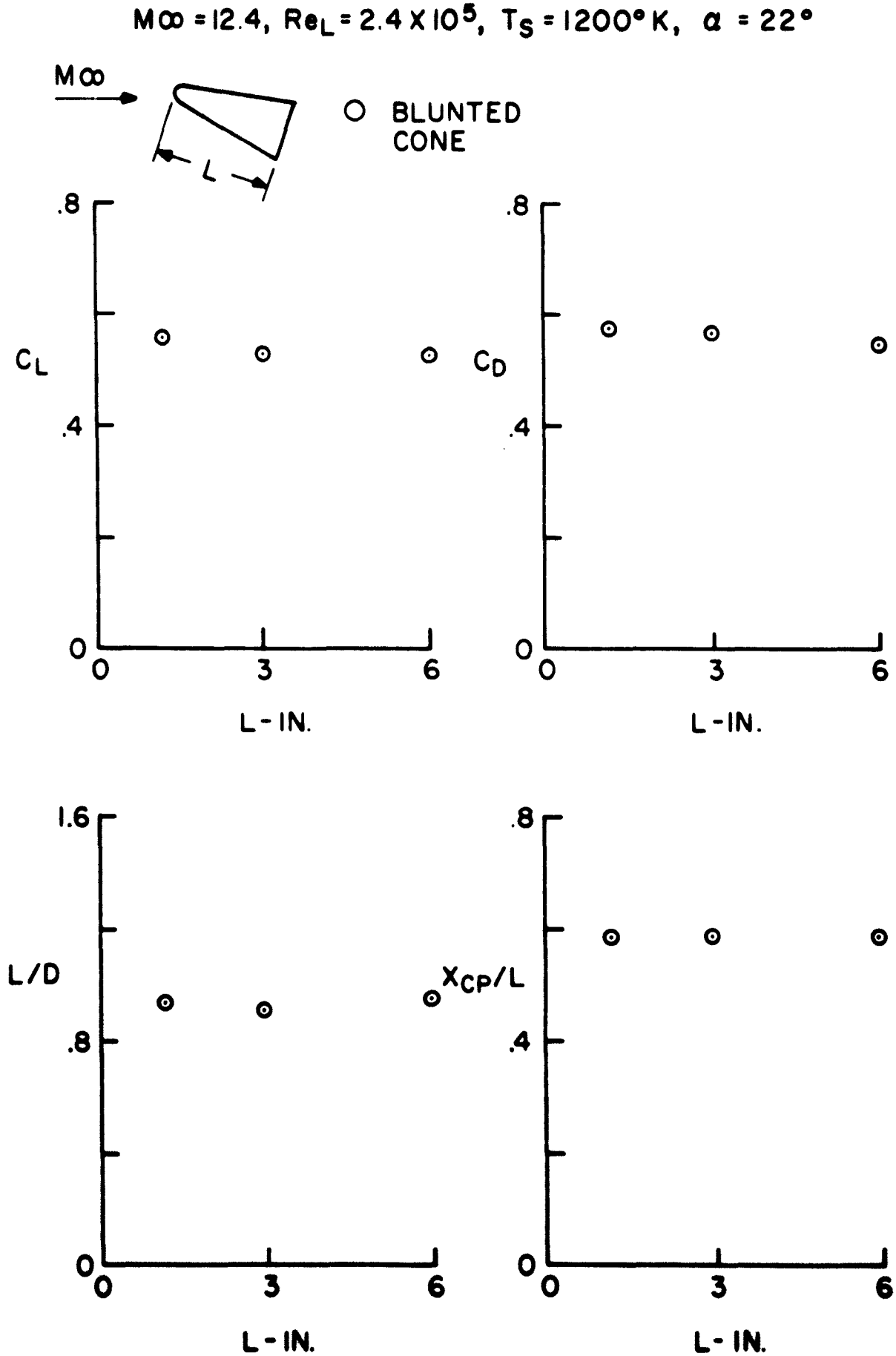

Figure 15. Effect of Flow Divergence on Model Force Data

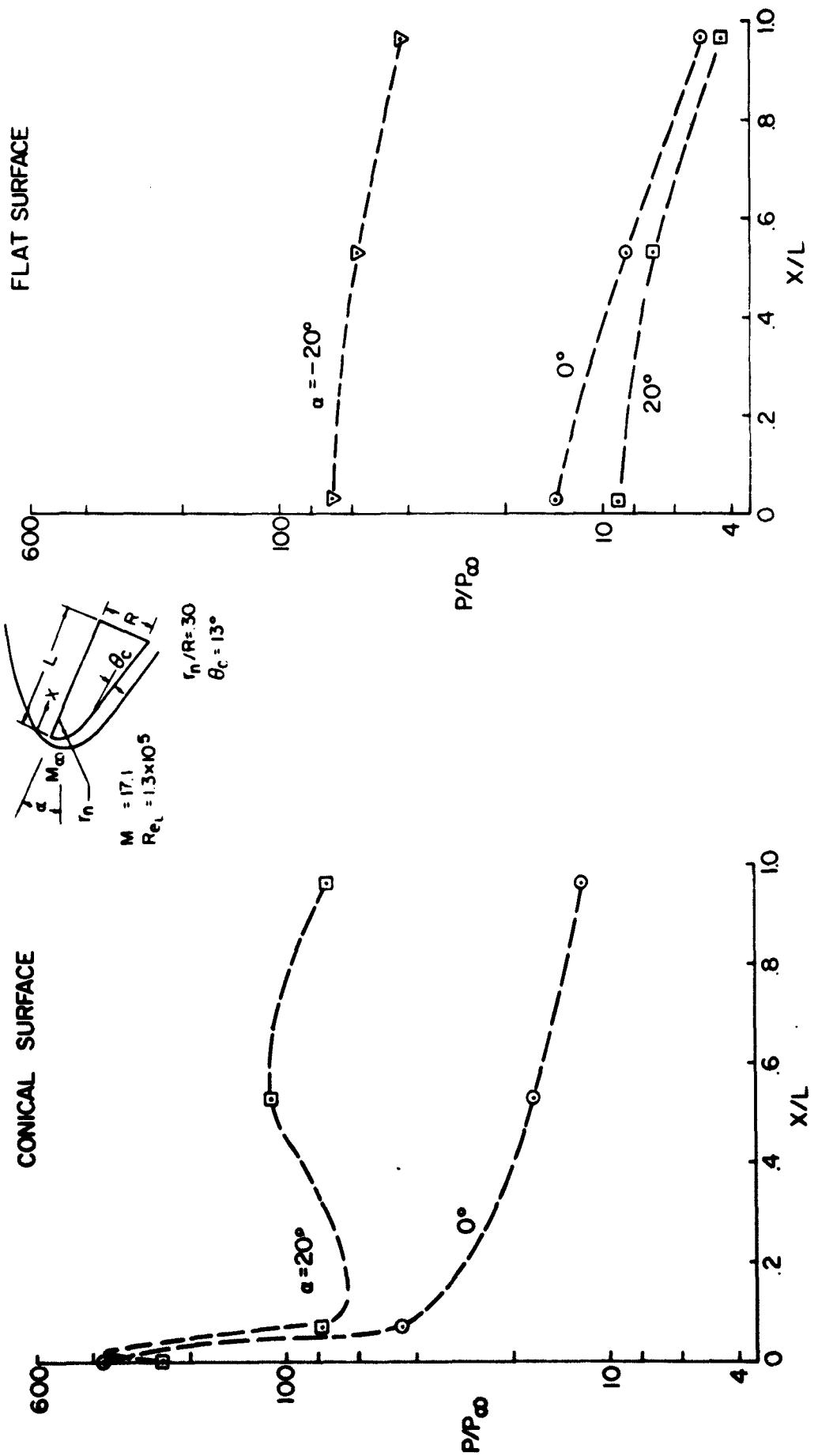

Figure 16. Pressure Distributions for a Half Sphere Cone Body

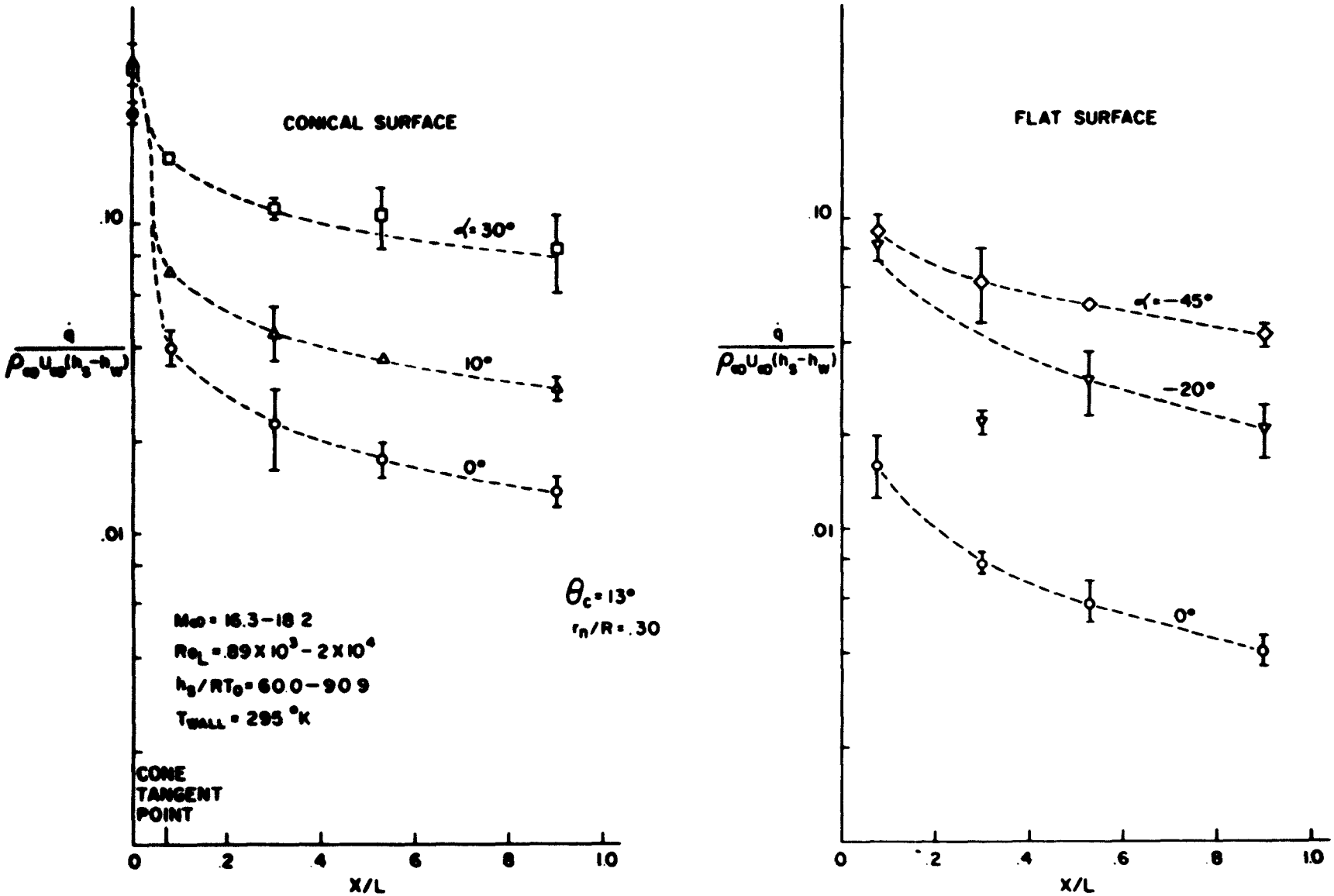

Figure 17. Heat Transfer Rate Distributions for a Half Sphere Cone Body

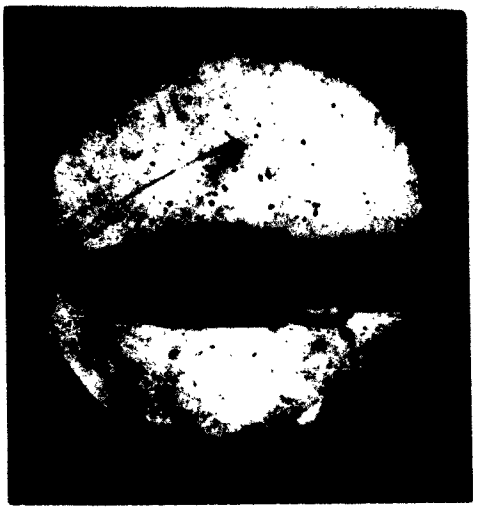

Figure 18a. Schlieren Photograph of Blunt Wedge
$\alpha = 0^\circ$
$M_\infty = 21.2$
$Re_\infty/in = 3.5 \times 10^4$
$Ts = 1500^\circ K$

Figure 18a. Schlieren Photograph of Blunt Wedge
$\alpha = 0^\circ$
$M_\infty = 4.6$
$Re_\infty/in = 7.7 \times 10^3$
$Ts = 5700^\circ K$

Figure 18b. Schlieren Photograph of Enlarged Nose Section of 13° Half Sphere Cone

$\alpha = -5^{\circ}$

$M_{\infty} = 12.4$

$Re_{\infty}/in = 1.4 \times 10^{5}$

$Ts = 1200^{\circ}K$

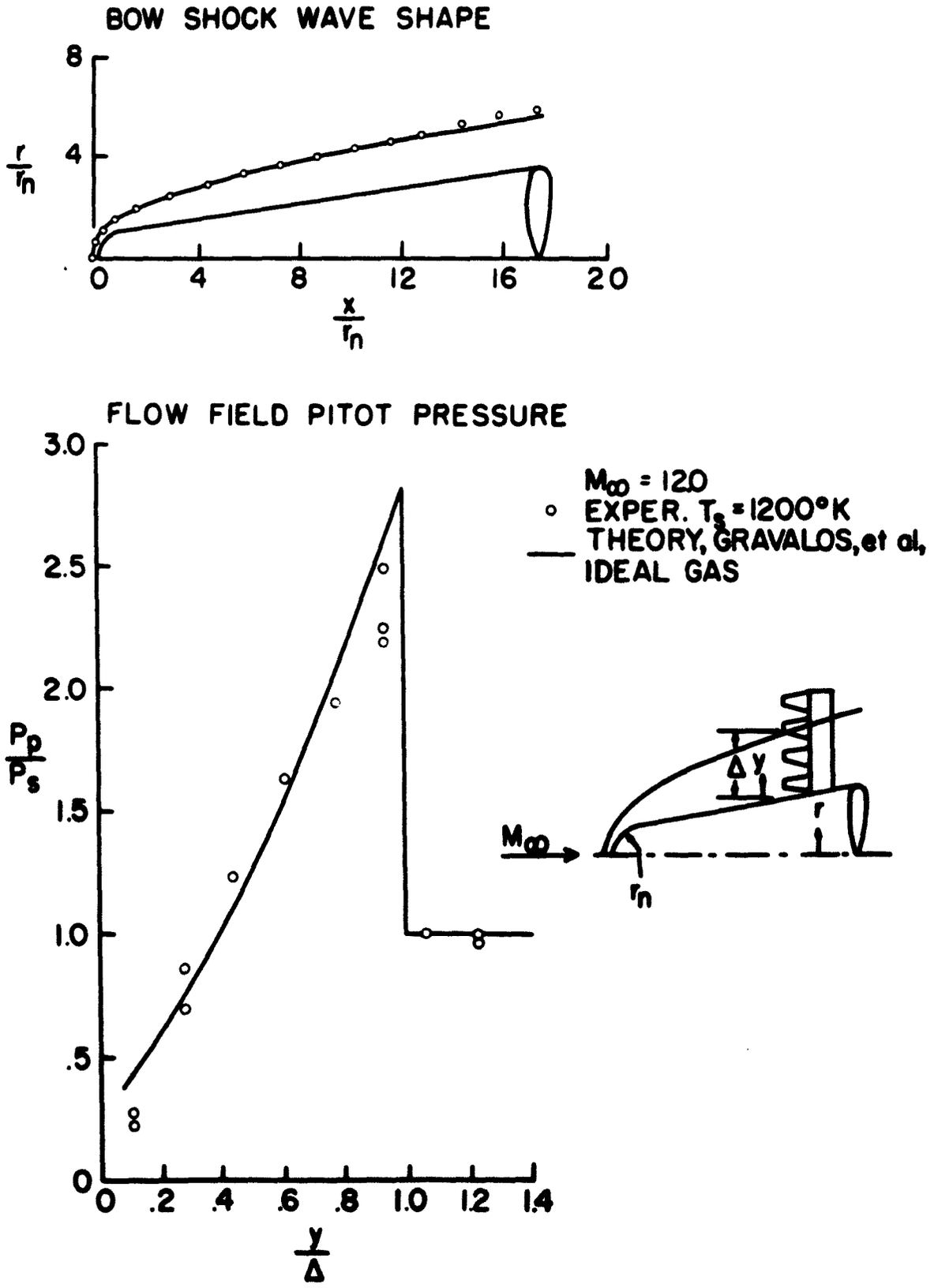

Figure 19. Comparison of Experiment and Theory for Blunted Cone

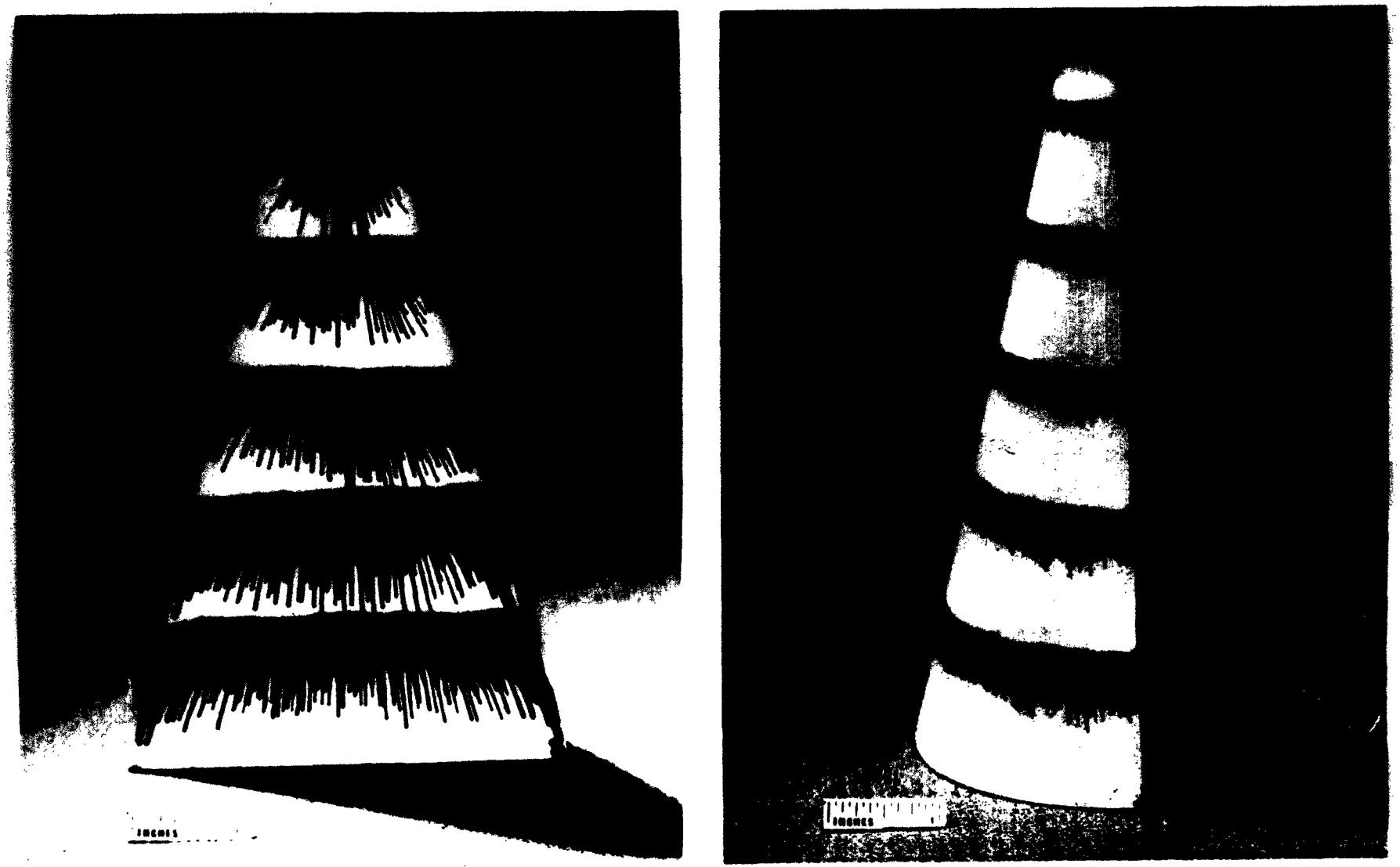

TOP VIEW

SIDE VIEW

Figure 20. Oil Streak Patterns on a Half Sphere Cone Body

$M_\infty = 12.1$ $Re_\infty/IN = 1.5 \times 10^5$ $\alpha = 0^o$

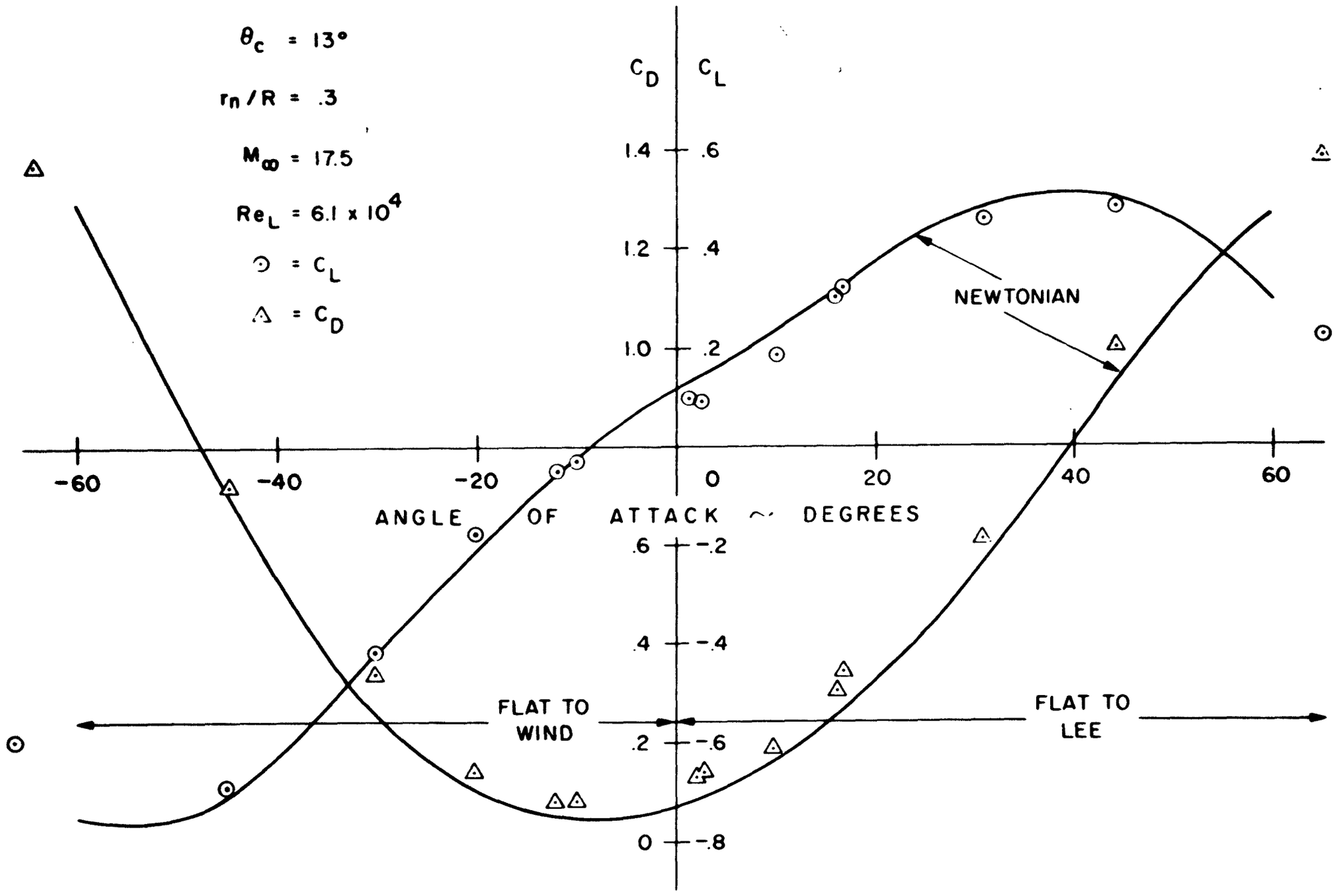

Figure 21a. Lift and Drag for a 13° Half Sphere Cone

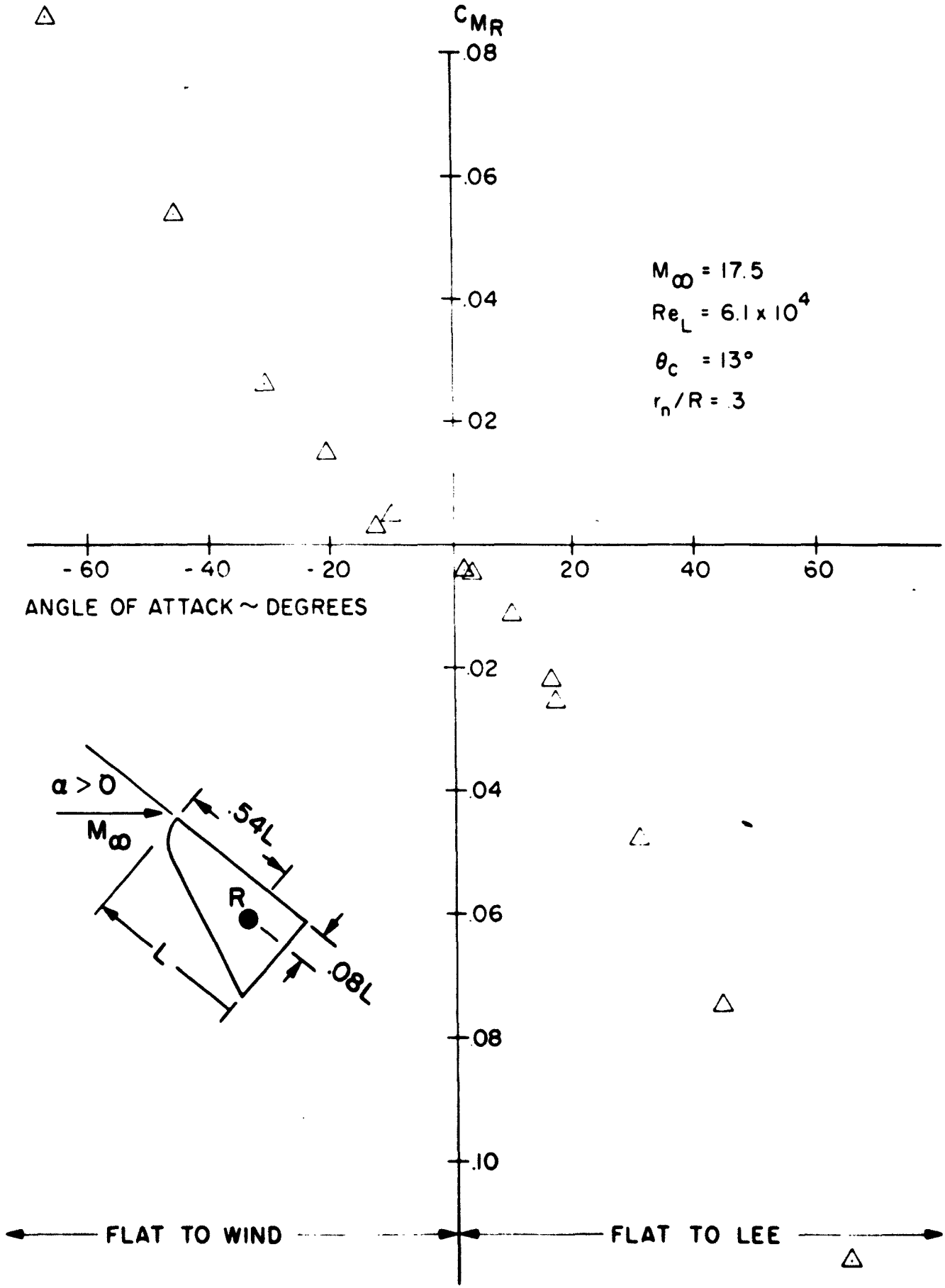

Figure 21b. Pitching Moment for a 13° Half Sphere Cone

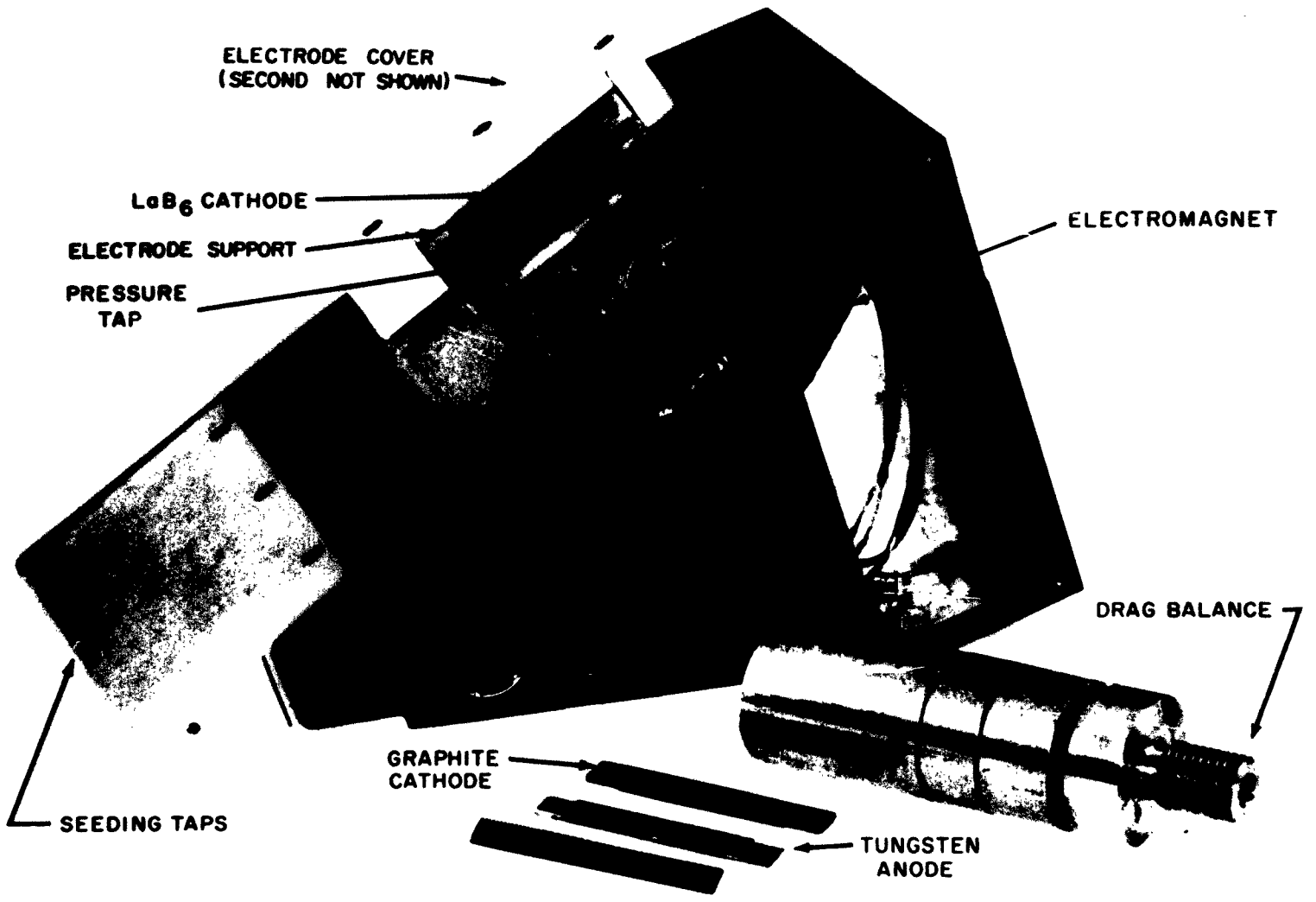

Figure 22. MHD Flight Attitude Control Model

GENERAL ELECTRIC

SPACE SCIENCES LABORATORY
MISSILE AND SPACE VEHICLE DEPARTMENT

TECHNICAL INFORMATION SERIES

AUTHOR	SUBJECT CLASSIFICATION	NO.
W. R. Warren et al.	Aerodynamics	R62SD56
		DATE: May, 1962

TITLE: SHOCK TUNNEL STUDIES OF THE AERODYNAMICS OF ATMOSPHERIC ENTRY

ABSTRACT: The capabilities of the shock tunnel in the study of the aerodynamics of atmospheric entry are discussed. Five major test instrumentation techniques and studies designed to investigate the quality of the test section flow are described. Recent results obtained in the G. E. M. S. V. D. shock tunnels are presented.

G. E. CLASS	REPRODUCIBLE COPY FILED AT	NO. PAGES
I	G. E. TECHNICAL INFORMATION CENTER 3198 CHESTNUT STREET PHILADELPHIA, PENNA.	47
GOV. CLASS: None		

By cutting out this rectangle and folding on the center line, the above information can be fitted into a standard card file.

AUTHOR W. R. Warren Jr., Clarence J. Harris, L. M. Kaegi, R. E. Lyon

COUNTERSIGNED C. Mannal

DIVISION Defense Electronics

LOCATION Valley Forge Space Technology Center, King of Prussia, Pa.